UNIVERSITÉ DU QUÉBEC

MÉMOIRE PRÉSENTÉ À

L'UNIVERSITÉ DU QUÉBEC À TROIS-RIVIÈRES

COMME EXIGENCE PARTIELLE

DE LA MAÎTRISE EN SCIENCES DE L'ÉNERGIE ET DES MATÉRIAUX

PAR

CAN TAO

BIOMASS BASE-FACILITATED AQUEOUS REFORMING FOR HYDROGEN PRODUCTION

JUILLET 2016

Résumé

Le reformage alcalin et aqueux (AAR-a*queous alkaline reforming*) est une technologie prometteuse pour la production d'hydrogène pur à partir de biomasse et sans émission de gaz carboniques. L'avantage principal de ce procédé est que, théoriquement, tout le carbone compris dans la biomasse est converti en carbonate de sodium (Na_2CO_3) qui a une certaine valeur commerciale. Le principe du procédé est essentiellement de recombiner la teneur en carbone de la biomasse via une réaction chimique pour former des carbonates et donc de libérer l'hydrogène dans a forme pure. L'hydrogène produit est pur à 95+ % et peut être utilisé directement dans certaines applications. La teneur en humidité de la biomasse ne modifie pas le procédé puisque de l'eau est nécessaire pendant le processus de conversion, évitant ainsi le besoin de sécher la biomasse. La réaction chimique décrivant ce procédé est :

$$(C_6H_{10}O_5)_n + 12n\ NaOH + n\ H_2O \xrightarrow{(Ni)} 6n\ Na_2CO_3 + 12n\ H_2O.$$

Cette réaction est optimum à des températures entre 300 et 350 °C.

Ce mémoire porte sur la conception d'un réacteur à lit fluidisé (FBR-*fluidized bed reactor*) et d'un banc d'essai pour produire de l'hydrogène de manière continue via le procédé d'AAR. Le banc d'essai comprend entre autres le FBR, un condensateur, un séparateur cyclonique, une pompe à recirculation et un contrôleur de débit. L'objectif du projet est d'accroitre la production d'hydrogène en expérimentant le FBR en mode de recirculation des gaz. La production d'hydrogène via l'AAR a déjà été étudiée dans un réacteur en mode continu. Contrairement au mode continu, la production d'hydrogène dans un FBR en recirculation ne subira pas d'augmentation drastique de pression. Les problèmes encourus du procédé AAR en mode continu ont été identifiés et discutés. Le catalyseur utilisé pour l'AAR a été produit expérimentalement en utilisant un procédé d'imprégnation de nitrate de nickel sur des billes d'alumine.

Le Chapitre 1 met en perspective le potentiel de la biomasse pour remplacer les carburants fossiles et contribuer de façon significative à l'atténuation de la pollution atmosphérique. La production d'hydrogène y est abordée ainsi que les différentes techniques connues. Les

objectifs du travail sont présentés à la fin du chapitre. Le Chapitre 2 présente une revue de la littérature sur le procédé d'AAR et sur les réacteurs à lit fluidisé.

La partie expérimentale et les éléments du banc d'essai pour le procédé d'AAR en mode continu sont introduits au Chapitre 3, soit en autres :

- Le réacteur à lit fluidisé (FBR) : Endroit où la cellulose subit le procédé d'AAR.
- Condensateur : Échangeur de chaleur pour condenser la vapeur qui s'échappe du FBR.
- Séparateur cyclonique : Retient les particules solides dans le flux du gaz en circulation.
- Contrôleur de débit massique : Sert à monitorer et contrôler le débit du gaz en circulation.
- Pompe: Compatible avec l'hydrogène et recircule le gaz dans le banc d'essai.

Plus particulièrement, la conception et les caractéristiques du FBR et du séparateur cyclonique ainsi que les paramètres importants pour obtenir la fluidisation y sont discutés. Le Chapitre 4 présente les résultats expérimentaux et la discussion, et le Chapitre 5 est la conclusion.

Les expériences ont été faites avec plusieurs débits de gaz en recirculation et différents catalyseurs. Nos résultats montrent que de l'hydrogène pur à 97.25 % a été produit sans traces de CO ni de CO_2 à une température de 623 K, avec 2 Moles de NaOH, en présence de catalyseur de Ni supporté et avec un débit de recirculation de 7 L/min. Le banc d'essai a aussi été modifié pour parer à la perte d'eau due à la condensation de la vapeur sur les parois des tuyaux et dans la pompe.

Abstract

Aqueous alkaline reforming is quite a good method to produce high purity of hydrogen without carbon dioxide emission. The principal advantage of this process is that theoretically, all the carbon in the biomass is converted into sodium carbonate (Na_2CO_3), a commercial product. The aqueous alkaline reforming was conducted in the fluidized reactor system that consists of a fluidized bed reactor, a condenser, a cyclone separator and a recirculating pump. The objective of conducting the experiment in a fluidized reactor is to increase the contact surface area between the reactants and water vapor to increase the hydrogen production efficiency. The experiments were conducted with different flow rates and catalysts, the gas produced was analyzed using a gas chromatography and the number of moles of hydrogen produced was calculated using the real gas equation. Our experiment results showed that hydrogen with a purity of 97.26 % was produced with no traces of either CO or CO_2 at a temperature of 623 K, with 2 Moles NaOH, in presence of supported Ni catalyst with a flow rate of 7 L/min. The system was also modified to avoid loss of water from condensed water vapor accumulated on the wall of the pipes and inside the pump.

Acknowledgement

Foremost, I would like to express my deepest gratitude to my supervisor Prof. Jean Hamelin for the continuous support of my master study and research, for excellent guidance, patience, motivation, caring, and immense knowledge. His guidance helped me in all the time of research and writing of this thesis.

I would like to thank Dr. Sadesh Kumar Natarajan for his encouragement, insightful comments and initial guidance which provide me with an excellent atmosphere for doing research. My sincere thanks also goes to Robert Drolet and Daniel Cossement for offering me help in building the system and leading me to work on the exciting project. I would express my sincere gratitude to Dr. Renju Zacharia for his technical support and stimulating discussions during the process of the project. I express my sincere thanks to my colleague Arulsamy Merly Xavier, for her wonderful co-operation and suggestions during the project. Also I thank my colleague Siyad Ubaid, Francis Lafontaine and Marie-Eve Marchand-Lamarche for their constant technical advice, their encouragement and support.

I take this opportunity to express gratitude to all of the members of Hydrogen Research institute for their help and support. I also thank my family members for the everlasting encouragement, support and attention.

The Financial support from BIOFUELNET Canada to Prof. Jean Hamelin was gratefully acknowledged.

Table of content

List of Figures

List of Tables

Nomenclature

h_i	Heat transfer coefficient of inner pipe (J/m^2 s K)
h_o	Heat transfer coefficient of annulus (J/m^2 s K)
ρ_p	Argon mass density (kg/m^3)
μ_p	Viscosity of argon flowing in the inner pipe (kg/ms)
C_P	Specific heat of argon flowing in pipe (J/kg K)
K_P	Thermal conductivity of the argon flowing in the inner pipe (J/s mK)
m	Mass flow rate of argon flowing in the inner pipe (kg/s)
d	Diameter of inner pipe (m)
ρ_a	Fluid mass density (kg/m^3)
μ_a	Viscosity of fluid flowing in the annulus (kg/ms)
K_a	Thermal conductivity of the fluid flowing in the annulus (J/s mK)
ω	Mass flow rate of fluid flowing in the annulus (kg/s)
C_{pa}	Specific heat of fluid flowing in the annulus (J/kg K)
μ_a	Viscosity of fluid flowing in the annulus (kg/ms)
μ_{wa}	Viscosity of fluid in the annulus at wall temperature (kg/ms)
D	Diameter of outer pipe (m)
r_o	Outside radius of the inner tube (m)
r_i	Inside radius of the inner tube (m)
k	Thermal conductivity of the stainless steel (J/s mK)
d_p	The diameter of catalyst (cm)
Ψ	Sphericity of the catalyst
ε_{mf}	Void fraction at the point of minimum fluidization (m/s)

d_t	Bed diameter (m)
ρ_c	Density of the catalyst (g/cm^3)
ρ_g	Density of the gas (g/cm^3)
μ	Viscosity of the gas (g/cm s)
P	Pressure of the inlet gas
u_{mf}	Minimum fluidization velocity (m/s)
u_t	Maximum velocity through the bed (m/s)
Q_m	Minimum flow rate (L/s)
Q_t	Maximum flow rate (L/s)

1 Introduction

1.1 Biomass as renewable energy

Hydrogen is a clean fuel and one of the most sustainable energy carriers [1]. However, today approximately 95% of hydrogen is produced from fossil fuels, with a huge quantity of carbon dioxide (CO_2) generated as a by-product. Emission of the carbon dioxide into the atmosphere [2] is responsible for the so-called "greenhouse gas effect (GHG)" which is having a severe impact on the environment, human health. Reducing the demand on fossil fuels is still a significant concern for many nations. Renewable-based processes like solar- or wind-driven electrolysis or photo-biological water splitting show great promise for clean hydrogen production. However, many advances still need to be made before these technologies can be economically competitive. For the near- and mid-term, generating hydrogen from biomass may be the more practical and viable, carbon neutral option for generating renewable hydrogen [3].

Canada is a country of over 9 million sq. km which has a large, well-developed forest sector and has historically been one of the world's largest exporters of wood products. Canada has vast biomass potential. Biomass is considered as one of the most abundant renewable energy resource [4]. It is formed by fixing carbon dioxide from the atmosphere during the process of plant photosynthesis [5], so biomass derived hydrogen can be assorted as carbon neutral because CO_2 released during hydrogen production is consumed by further biomass growth [6]. Biomass resources which can be used to convert to energy can be divided into four general categories [7]:

(1) Energy crops: herbaceous energy crops, woody energy crops, industrial crops, agricultural crops and aquatic crops.

(2) Agricultural residues and waste: crop waste and animal waste.

(3) Forestry waste and residues: mill wood waste, logging residues, trees and shrub residues.

(4) Industrial and municipal wastes: municipal solid waste, sewage sludge and industry waste.

1.2 Hydrogen production from biomass

The major pathways to convert biomass to hydrogen are shown in Figure 1.1 [8]; there are three major thermochemical approaches: pyrolysis, steam/oxygen gasification, and high-pressure water/steam treatment.

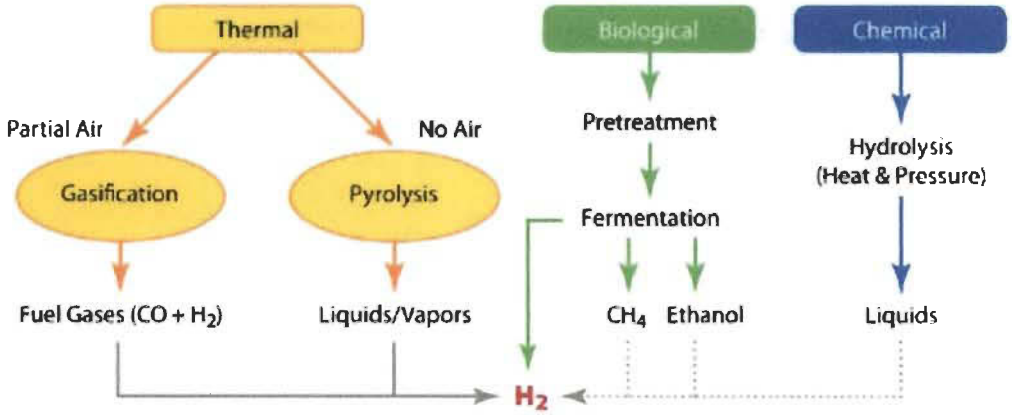

Figure 1.1: Biomass-to-hydrogen pathways.

1.2.1 Pyrolysis

Pyrolysis is the thermal conversion of biomass to liquid oil, solid charcoal and gaseous compounds by heating the biomass at a given temperature between 375 and 525 K for pressures ranging between 0.1 and 0.5 MPa in the absence of air [5]. Pyrolysis can also be classified as slow or fast process. The main by-product of slow pyrolysis is charcoal which is not considered for hydrogen production. Fast or flash pyrolysis can be chosen to produce hydrogen directly if temperature and sufficient volatile phase residence time are provided. The reaction equation is as follows:

$$C_XH_yO_2 + \text{heat} \rightarrow H_2 + CO + CH_4 + HCs, \quad (1)$$

where HCs stand for hydrocarbons. The methane and hydrocarbons can be reformed by steam to yield additional hydrogen when the water and gas shift reaction are used to increase hydrogen production. The water and gas shift reaction equations are as follows:

$$CH_4 + HCs + H_2O \rightarrow CO + H_2, \quad (2)$$

$$CO + H_2O \rightarrow CO_2 + H_2. \quad (3)$$

Besides the fuel gas, the bio-oil products can also be processed for hydrogen production by catalytic steam reforming. Figure 1.2 illustrates the energy products from pyrolysis [9].

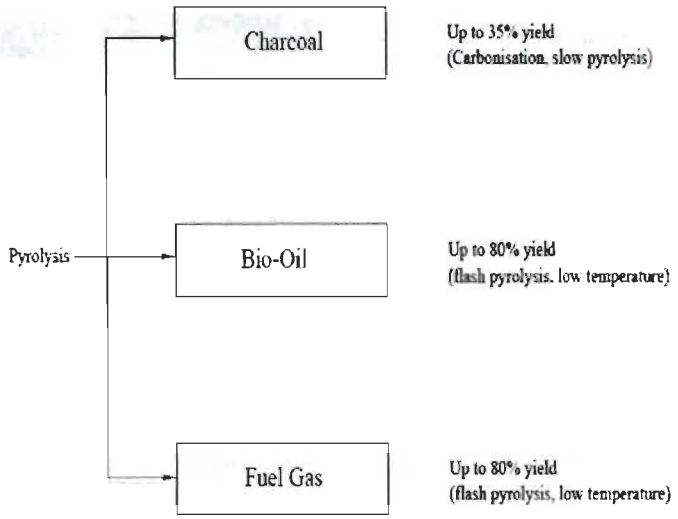

Figure 1.2: Energy products from pyrolysis.

1.2.2 Gasification

Gasification is a process that converts biomass to a combustible product gas or syngas (from synthesis gas or synthetic gas) at temperature above 1000 K by using various gasifying agents such as air, O_2, steam and/or their mixtures. There are several reactions during biomass gasification process: drying to evaporate moisture, pyrolysis to produce gases, vaporized tars or oils and a solid char residue, and gasification or partial oxidation of the residual char, pyrolysis tars and pyrolysis gases [10]. Major reactions [11] are included in the

Table 1.1. This process is more favourable for hydrogen production than pyrolysis, however, the presence of condensable organic compounds and methane in the product gas not only cause blockages and corrosion for the reactors but also limit the utilisation of the gas for specific applications which reduce overall efficiency, moreover, the gas cleaning technology is still the bottleneck for advanced gas utilization [12].

Table 1.1: Major reactions in biomass gasification process.

Stoichiometry	Heat of reaction (kJ/mol)	Name
Biomass → char + tar + H_2O + light gas (CO + CO_2 + H_2 + CH_4 + C_2 + N_2 + ...)	>0	Biomass devolatilization
Char combustion		
$C_2 + \frac{1}{2}O_2 \rightarrow CO$	−111	Partial combustion
$C + O_2 \rightarrow CO_2$	394	Complete combustion
Char gasification		
$C + CO_2 \rightarrow 2CO$	+173	Boudouard reaction
$C + H_2O \rightarrow CO + H_2$	+131	Steam gasification
$C + 2H_2 \rightarrow CH_4$	−75	Hydrogen gasification
Homogeneous volatile oxidation		
$CO + \frac{1}{2}O_2 \rightarrow CO_2$	−283	Carbon monoxide oxidation
$H_2 + \frac{1}{2}O_2 \rightarrow H_2O$	−242	Hydrogen oxidation
$CH_4 + 2O_2 \rightarrow CO_2 + 2H_2O$	−283	Methane oxidation
$CO + H_2O \rightarrow CO_2 + H_2$	−41	Water–gas shift reaction
Tar reactions (tar assumed C_n and m)		
$C_nH_m + (n/2)\,O_2 \rightarrow nCO + (m/2)\,H_2$		Partial oxidation
$C_nH_m + n\,CO_2 \rightarrow (m/2)\,H_2 + (2n)\,CO_2$		Dry reforming
$C_nH_m + nH_2O \rightarrow (m/2+n)\,H_2 + nCO_2$	Highly endothermic +(200 to 300)	Steam reforming
$C_nH_m + (2n - m/2)\,H_2 \rightarrow n\,CH_4$		Hydrogenation
$C_nH_m \rightarrow (m/4)\,CH_4 + (n - m/4)\,C$		Thermal cracking

1.2.3 Sub- or supercritical water gasification of biomass for hydrogen production

Sub- or supercritical water has received considerable attention as a reaction medium for reforming wastes which is suitable to convert wet biomass to gases or other bio-based chemicals. The important advantage of this processing method over the other ones is its ability to use wet substrate without prior dewatering [13]. Supercritical water is obtained at pressures above 22.1 MPa and temperatures above 647 K. In the absence of oxygen, biomass is converted under supercritical water conditions into fuel gases, which are easily separated from the water phase by cooling to ambient temperature. The reaction is:

$$C_XH_yO_z + (2x - z)H_2O \rightarrow xCO_2 + \left(2x - z + \frac{y}{2}\right)H_2. \quad (4)$$

During the gasification of biomass in sub- or supercritical water, numerous reactions can occur in parallel in the system, e.g. hydrolysis, dehydration, decarboxylation, aromatization, condensation, depolymerisation/polymerization, hydrogenation/dehydrogenation, rearrangements, isomerization reactions, etc.

Among the methods mentioned above, hydrogen can be produced from biomass, but the reaction process is complex and mostly the product gas contains CO, CO_2 and trace amount of other gas or the gas needs to be further purified through the other process. In order to broaden the choices of the resources and the basic technologies, an innovative method for the one-step production of hydrogen without CO and CO_2 is strongly desired.

1.3 Research objectives

Production of hydrogen with zero emissions of carbon is an ideal way. Ultra-high pure hydrogen production is an expensive process that requires considerable use of gas purification systems. If hydrogen production and carbon sequestration can both take place in the same reactor, it will be more energy efficient. In our reactor CO_2 is sequestered by the reactant sodium hydroxide which produces sodium carbonate, therefore only high purity hydrogen is produced.

We have already demonstrated the experiment successfully in a batch scale reactor. For the batch reactor, the energy consumption is high. In order to improve hydrogen production from the biomass as well as reduce the energy consumption, we run the system in the fluidized reactor where the flow velocity generated by the circulating the pump increases the surface contact area between the reactants and water vapour. Furthermore, the fluidized reactor provides more flexible reactants loading which can be applied at an industry scale.

The experiments were conducted in the fluidized bed with different flow rates. The system was modified to avoid the condensed water inside the system. The produced gas was analyzed using a gas chromatography and the number of moles of hydrogen produced was calculated using the real gas equation.

The entire experimental study was classified in three parts. The pre-test was conducted to control the heating process and monitor temperature distribution inside the fluidized reactor. Reactions in the fluidized reactor with circulating pump at different flow rates were performed to get the optimal parameters for hydrogen production. Due to the accumulated water in the system during the circulating process which reduces the hydrogen production, the reactor was modified several times to solve the problem.

2 Literature review

2.1 Aqueous alkaline reforming

In 2003, S.K. Saxena [14] calculated thermochemical equilibrium in the system Na–C–H–O, it is shown that carbon or methane, water and sodium hydroxide can be used in appropriate molar proportions to produce almost pure hydrogen and solid sodium carbonate. The reaction in a multicomponent thoroughly stirred system of sodium hydroxide, carbon or methane and water at 1 atm and temperature from 525.15 K to 773.15 K results in almost pure hydrogen and the by-product sodium carbonate. The dual role of sodium hydroxide is to contribute a hydrogen atom to the final gas as well as to produce sodium carbonate from the nascent CO or CO_2. One step hydrogen production from carbonaceous compounds is desirable. Later, Ishida *et al.* [15] proposed that CO- and CO_2-free hydrogen can be produced from the reaction between biomass (cellulose, sucrose, glucose, starch, cotton, or paper) and sodium hydroxide in the presence of water vapor at temperature range from 473 to 623 K under atmospheric pressure. The reaction can be written as follows:

$$(C_6H_{10}O_5)_n + 12NaOH + H_2O \rightarrow 6Na_2CO_3 + 12H_2.$$

They also investigated the effects of catalyst Ni, Co, Rh, or Ru supported on Al_2O_3 on the reaction. Without catalyst, total yield of hydrogen obtained through the reaction at a temperature range 473-773 K was 62%. However, the formation of hydrogen was specifically enhanced by catalyst addition that the total hydrogen yield was dramatically improved to 100% on the basis of the stoichiometric equation. They speculated that Ni, Co, Rh, and Ru catalysts promote cleavage of C-H bonds of cellulose derivatives, intermediate reactions, and desorption of H species as H_2 to the gas phase [16].

In 2010, a company called Energy Conversion Device developed a new technology to produce hydrogen from various organic matters which were renewable fuels including liquid biofuels and solid biomass materials. Sodium hydroxide was used as the base materials to facilitate the reforming. In comparison with the reaction of conventional steam reforming, this one-step process showed number of advantages including lower operation temperature (403 to 573 K) and lower heat consumption because of the lower heat of reaction (enthalpy). The only by-

product sodium hydroxide can easily be separated and reacted to regenerate using the well-known pulp and paper Kraft process [17].

3 Experimental

3.1 Reactants

$$(C_6H_{10}O_5)_n + 12n\ NaOH + n\ H_2O \xrightarrow{catalyst} 6n\ Na_2CO_3 + 12n\ H_2$$

The reactants which were used in the experiment are as follows: cellulose (from paper and pulp center), sodium hydroxide (Sigma Aldrich, reagent grade, >98%, pellets), deionized water and commercial catalyst: supported nickel catalyst (~65wt.% on silica/alumina) and pure nickel catalyst (power, 3~micron, 99.7%).

In this reaction, one mole of cellulose (162 g) reacts with 12 moles of NaOH (12×40 g) and 1 mole of H_2O (18 g) in presence of catalyst to produce 6 moles of Na_2CO_3 (6×106 g) and 12 moles of H_2 (12×2g) according to the stoichiometry.

3.2 Catalyst preparation

The catalysts were prepared using the support impregnation method. The alumina balls with size range of 2-3 mm were selected, nickel nitrate hexahydrate (Sigma Aldrich, 99.999%, trace metals basis) was used for the support impregnation. 3 g of alumina balls were soaked in 10 ml 1 mol/L nickel nitrate solution for 4 h and drying in an oven at 413.15 K overnight, then calcining in air. In order to control the nitrate decomposition more carefully, the precursors were maintained at 573.15 K for 3 h and then the Ni/Al_2O_3-B catalyst was calcined at the final temperature of 1123.15 K for 5 h. Before we started the experiment, the Ni/Al_2O_3-B catalyst was reduced in the hydrogen flow at 973.5 K for 3 h to get the reduced Ni/Al_2O_3-B.

3.3 Analyzing methods

The structures of the catalysts are analyzed through X-ray diffraction (XRD) with a Brucker diffractometer model D8 Focus using Cu Kα – X-ray source operation at room temperature.

A MicroGC model 3000 from Agilent Technologies with a Molecular Sieve 5A column (for separating neon, hydrogen, oxygen, nitrogen, methane and carbon monoxide) and a PLOT U

column (for separating carbondioxide, ethylene, ethane, acetylene) is used to detect the produced gas. The MicroGC is calibrated using a universal gas calibration standard (

Table 3.1). Agilent Certify software is used to control the MicroGC runs.

Table 3.1: The universal gas calibration standard.

Components	Concentration
Helium	0.10%
Neon	0.05%
Hydrogen	0.10%
Oxygen	0.055%
Nitrogen	0.105%
Methane	Balance,99.05%
Ethane	0.05%
Ethylene	0.05%
Carbon dioxide	0.050%
Carbon monoxide	0.10%
Acetylene	0.05%
Propane	0.05%
Methyl Acetylene	0.05%
n-Butane	0.05%
n-Hexane	0.05%
n-Heptane	0.05%

3.4 Experiment apparatus

3.4.1 Thermocouple

Thermocouple (OMEGA ® Quick Disconnect Molded Thermocouple, KQSS-14G-6) with stainless sheath diameter of 1/4" is used to monitor the temperature variation during the circulating process in several points of the system.

The multipoint thermocouple which is used to monitor the temperature variation inside the main reactor is shown in the Figure 3.1. The temperatures K1, K2, K3, K4 and K5 are the temperature values measured at the multipoint 0, 2, 4, 6 and 9, respectively as shown in Figure 3.1.

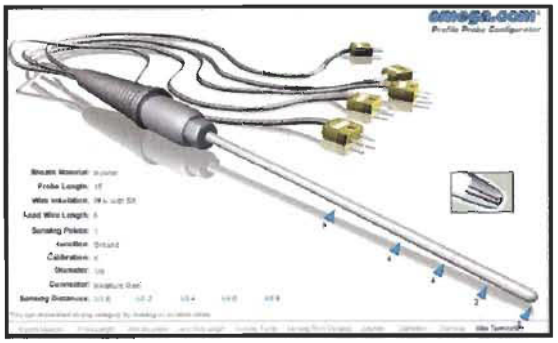

Figure 3.1: Multipoint thermocouple.

3.4.2 Pressure transducer

A pressure transducer is a transducer that converts pressure into an analog electrical signal. Although there are various types of pressure transducers, one of the most common is the strain-gage base transducer. The conversion of pressure into an electrical signal is achieved by the physical deformation of strain gages which are bonded into the diaphragm of the pressure transducer and wired into a wheatstone bridge configuration. Pressure applied to the pressure transducer produces a deflection of the diaphragm which introduces strain to the gages. The strain will produce an electrical resistance change proportional to the pressure. Since a 4-20mA signal is least affected by electrical noise and resistance in the signal wires, these transducers are best used when the signal must be transmitted long distances. The pressure transducer we used is from Omega, the pressure range is from 0-1,000 psi with 4-20 mA output as showed in Figure 3.2.

Figure 3.2: Pressure transducer.

3.4.3 Heaters

Three band heaters which are used to heat the reactor are from Tempco, the parameters are shown in Table 3.2.

Table 3.2: The parameters of band heaters.

mica band heater	size (ID×W FT^2)	voltage and current	capacity
1	3×5	125V 15A	1200 W
2	3×3	125V 15A	1000 W
3	3×2	125V 15A	500 W

The flexible heating tape is from omega (SRT051-060) with the heating capacity of 156 W and current of 1.3 A. The size is 0.5×6 FT.

3.4.4 PID controller and solid state relay

The temperature of the reactor is regulated by a PID based on the data acquired by thermocouple fitted on to the heating element. The wiring schematic of PID (Omega, CN7533) with the solid state relay (SSRL 240 AC 25) is given in Figure 3.3.

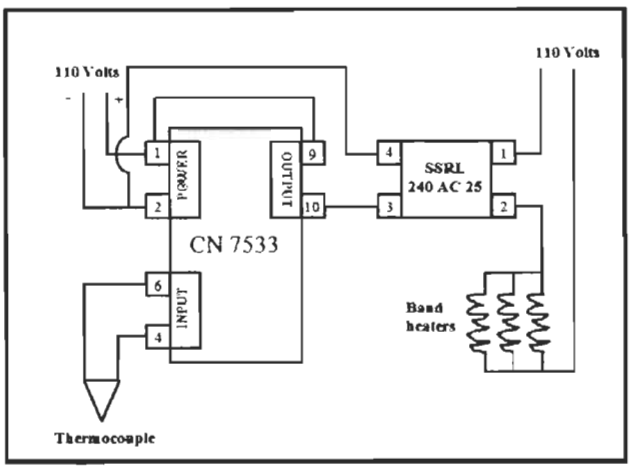

Figure 3.3: The wiring schematic of PID and solid state relay.

3.4.5 Pump

Quad head explosion proof pump is used as showed in Figure 3.4. The pump can be connected in parallel, series or parallel combined with series depending on the maximum pressure, vacuum or the flow rate as shown in Figure 3.5. In our system parallel connection is used to achieve the maximum flow rate of 110 SLPM.

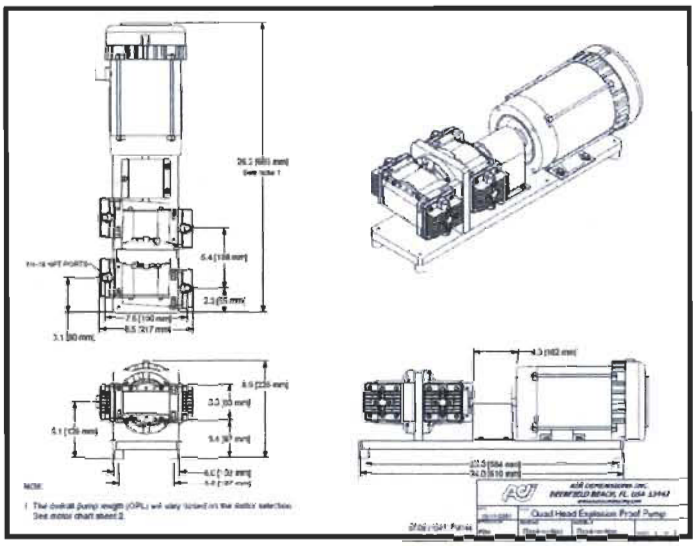

Figure 3.4: Design of the pump.

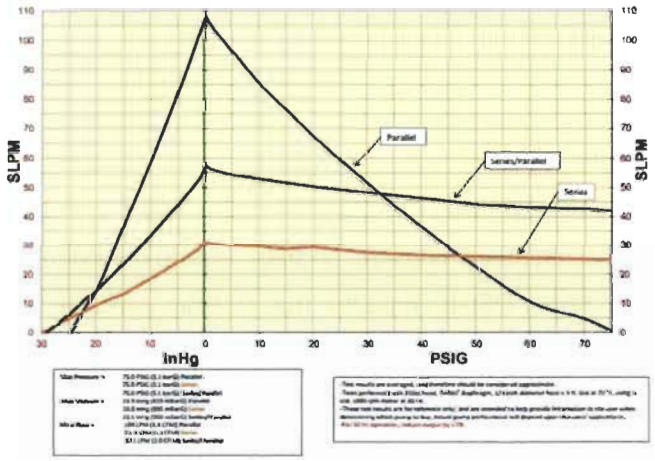

Figure 3.5: Performance curve of the pump.

3.4.6 Mass flow controller

Mass flow controller from Aalborg (GFC 77) is used to control the flow rate for the system. The stream of gas entering the Mass Flow transducer is split by shunting a small portion of the flow through a capillary stainless steel sensor tube. The remainder of the gas flows through the primary flow conduit. The geometry of the primary conduit and the sensor tube are designed to ensure laminar flow in each branch. According to principles of fluid dynamics flow rates of gas in two properly sized laminar flow conduits are related to one another. Therefore, the flow rates measured in the sensor tube are directly proportional to the total flow through the transducer. In order to sense the flow in the sensor tube, heat flux is introduced at two sections of the sensor tube by means of precision wound heater-sensor coils. Heat is transferred through the thin wall of the sensor tube to the gas flowing inside. As gas flow takes place heat is carried by the gas stream from the upstream coil to the downstream coil windings. The resultant temperature dependent resistance differential is detected electronically. The measured gradient at the sensor windings is linearly proportional to the instantaneous rate of flow taking place. An output signal is generated that is a function of the amount of heat carried by the gases to indicate mass-molecular based flow rates. GFC Mass Flow Controller model GFC77 incorporates a motorized valve. The closed loop control circuit of the GFC continuously compares the mass flow output with the selected flow rate. Deviations from the set point are corrected by compensating valve adjustments, thus maintaining the desired flow parameters. The flow rate range is 0-600 SLPM, gaseous argon was used for calibration and the maximum pressure is 500 psi.

3.4.7 Nl instruments

NI 9207 (16 Channels, ±20 mA/±10 V, 24-Bit analog input module) serves as the input modules for the temperature and pressure. NI 9207 is powered externally by a 15 V power supply which has a 37-pin DSUB connector that provides connections for 16 analog input channels: 8 voltages and 8 currents. In this system, the input current in mA as per the pressure variation is used to monitor the pressure change. For connecting an external power supply, one of the nine V_{sup} pins is connected with the positive terminal of the external power supply and

one of the COM is connected to the negative terminal of the power supply as is shown in Figure 3.6.

Each current channel has an AI pin to connect a current signal. The NI 9207 has AI 8-AI 15 for current input signal. AI pin is connected to black wire (negative input) of the pressure transducer and one of the V_{sup} pins is chosen to connect the red wire (positive input) of the pressure transducer for collecting pressure data.

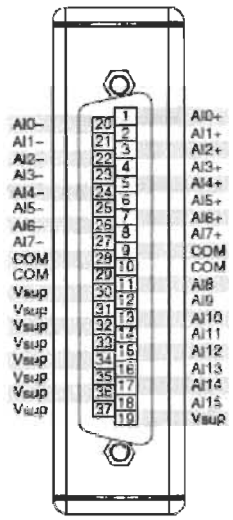

Figure 3.6: NI 9207 Pin Assignments.

The NI 9213 is used to collect the temperature data from the thermocouples. It has a 36-terminal detachable spring-terminal connector that provides connections for 16 thermocouple channels. For the thermocouple connection, connect the positive lead of the thermocouple to the TC+ terminal and the negative lead of the thermocouple to the TC– terminal as is shown in Figure 3.7.

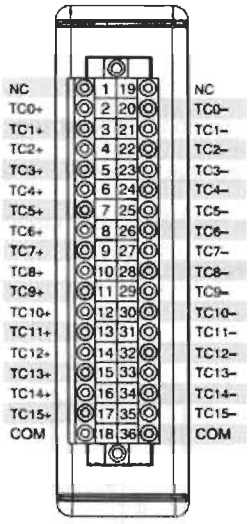

Figure 3.7: NI 9213 Terminal Assignments.

3.4.8 Labview

The data from the system during the experimental reaction is acquired and monitored using Labview 9.0 version. LabVIEW is commonly used for data acquisition, instrument control, and industrial automation on a variety of platforms. It is a graphical interface that allows the measurement, test and control of the whole setup, the Front panel and block diagram of Labview for this system are given in Figure 3.8. In the front panel, there are three pressure indicators which monitor the pressure changes in different part of the system and the diagram showing the pressure changes with time. Also, there are eight thermometers which track the temperature changes in different point of the system and the diagram showing the temperature changes with time. The block diagram shows the programing process.

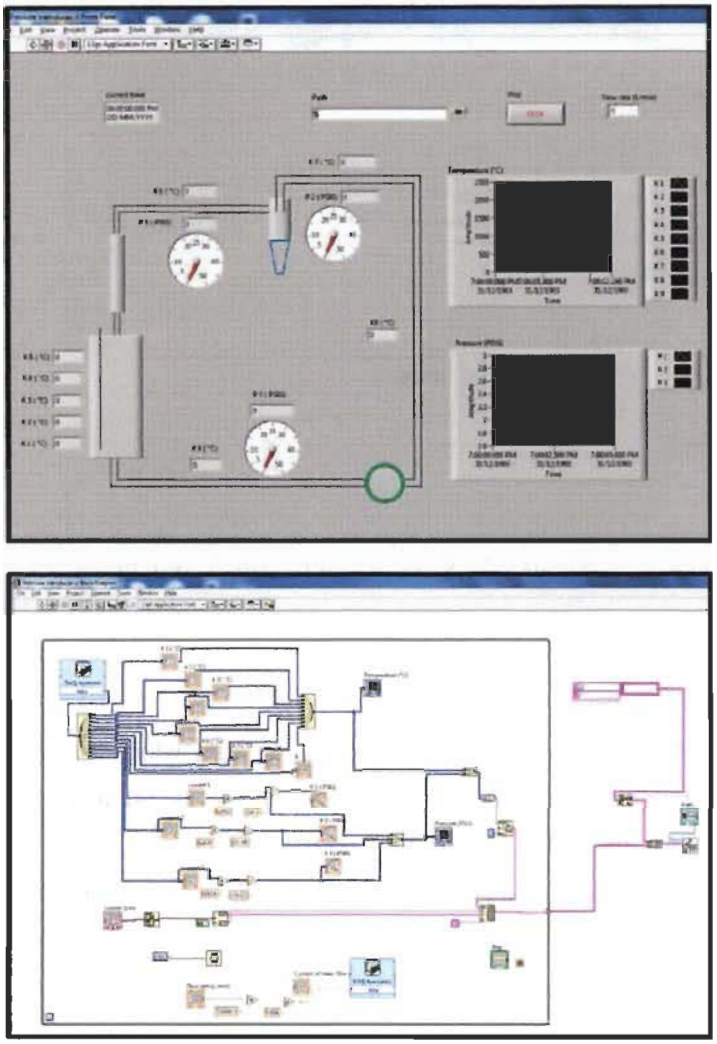

Figure 3.8: Front panel and block diagram of Labview.

3.5 Experiment setup

The experimental setup is composed of a fluidized bed reactor, condenser, cyclone separator, mass flow controller and pump. The schematic of the whole system is shown in Figure 3.9 (the green colour part).

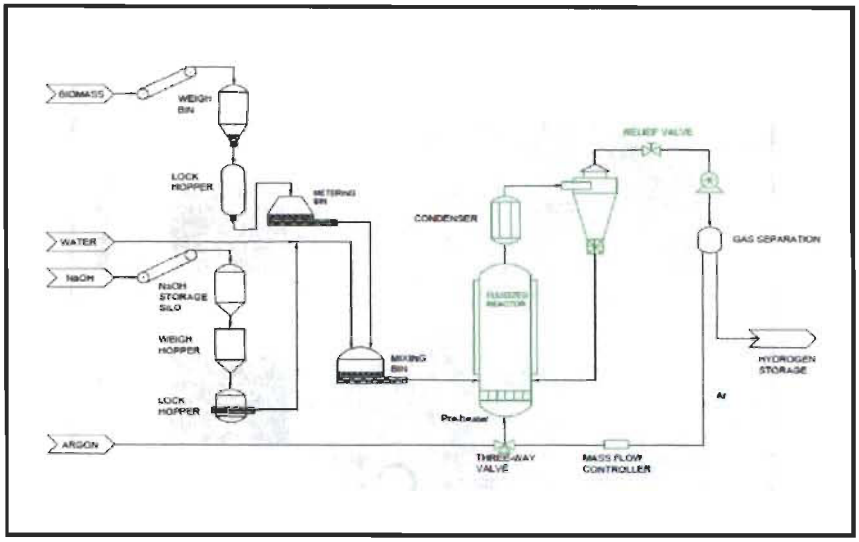

Figure 3.9: Schematic of the whole system.

3.5.1 Fluidized bed reactor

The fluidized bed reactor body is made of Inconel, an alloy which has high Nickel content. This Ni based alloy offers high resistance to caustic stress corrosion cracking and hydrogen embrittlement due to the ability of Ni to form protective stable oxides and hydroxides in high pH environments which acts as a protective passive film. The reactor is 21 inch height with a 2 inch ID which is shown in Figure 3.10. The reaction is carried out inside the reactor, all the reactants: cellulose, sodium hydroxide and the catalysts are supported by a distribution plate located at the bottom flange of the reactor which provides easy loading and removing of catalyst on the distributor plate. Sieve (Metal sifter) (Figure 3.10) is used as distribution plate. It is tightly attached to the column with the press of the gasket to avoid leaking.

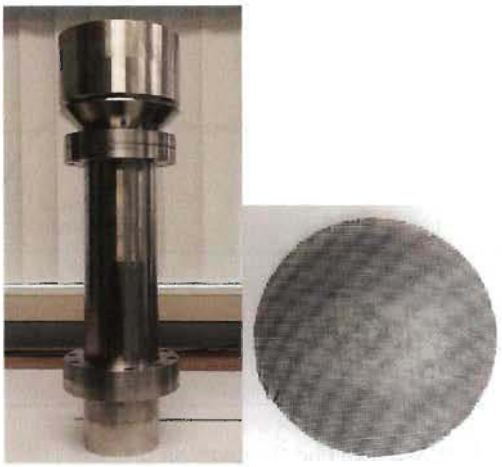

Figure 3.10: Fluidized bed reactor and distribution plate.

3.5.1.1 Particle size characterisation and calculation of fluidized velocity

The fluidized-bed reactor has the ability to process large volumes of fluid. Fluidization occurs when small solid particles are suspended in an upward flowing stream of fluid. The fluid velocity is sufficient to suspend the particles, but it is not large enough to carry them out of the vessel. The solid particles swirl around the bed rapidly, creating excellent mixing among them. The material "fluidized" is almost always a solid and the "fluidizing medium" is either a liquid or gas. The characteristics and behavior of a fluidized bed are strongly dependent on both the solid and liquid or gas properties.

Fluidization will be considered to begin at the gas velocity at which the weight of the solids gravitational force exerted on the particles equals the drag on the particles from the rising gas. All parameters at the point where these two forces are equal will be characterized by the minimum fluidization velocity (u_{mf}) to denote that this is the value of a particular term when the bed is just beginning to become fluidized. If the gas velocity is increased to a sufficiently high value, however, the drag on an individual particle will surpass the gravitational force on the particle, and the particle will be entrained in a gas and carried out of the bed. The point at which the drag on an individual particle is about to exceed the gravitational force exerted on it is called the maximum fluidization velocity u_t. These two situations are shown in Figure 3.11.

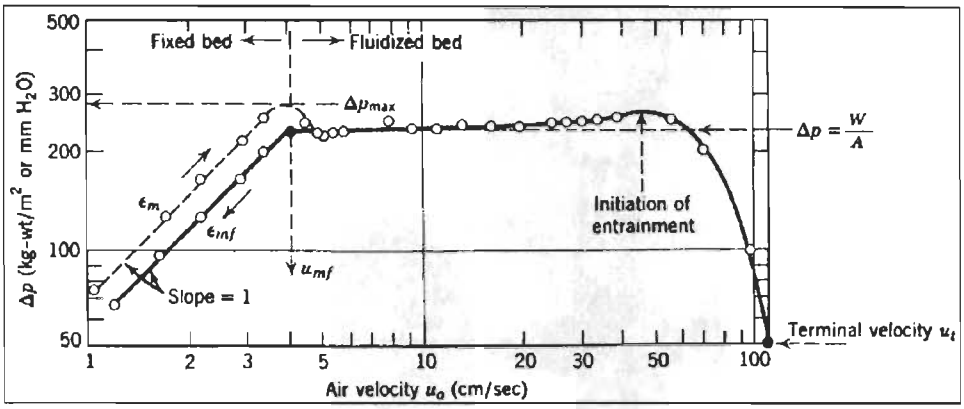

Figure 3.11: The fluidization process [18].

In order to control the flow rate, the minimum and maximum fluidization velocity are calculated, the parameters of the catalyst and the gas are shown in Table 3.3. The calculation is given in Appendix A.

Table 3.3: The parameters of the catalyst.

Symbol	Characterisation		Unit
d_p	diameter of catalyst	0.1	cm
ρ_c	density of the catalyst	1.5	g/cm^3
ρ_g	density of the gas	1.7×10^{-3}	g/cm^3
P	pressure of the inlet gas	14.7	psi
M_g	molecular weight of gas	40	m/s
d_t	bed diameter	26.8×10^{-3}	m
μ	viscosity of the argon gas	3.79×10^{-4}	g/cm/s
T	temperature of the argon gas	573	K

3.5.2 Condenser

A water cooled condenser which connects the reactor with cyclone separator is designed to cool the hot gas and keep the moisture content inside the reactor. The detailed design of the double pipe heat condenser is given in Appendix B.

3.5.3 Cyclone separator

Cyclones, which can separate the particles from an air stream, have been widely used in many industrial processes, such as air pollution control and environmental cleaning processes due to their well adaptability to harsh conditions, simplicity to design, and low costs to operate and maintain. The cyclone designs are generally classified into straight-through, uni-flow, and reverse-flow cyclones according to the purpose in use. Among them, it is known that the use of tangential inlet and reverse-flow is the most common way for cyclone design.

The schematic of the cyclone separator and the generated grid system are given in Figure 3.12 and the geometrical dimensions are depicted in Table 3.4. As can be seen in Table 3.4, all dimensions are normalized by using the diameter of cyclone body (D = 3.14 inch). According to the cyclone's height, it can be divided into three parts such as vortex finder (annular space), separation space and dust collection part. The inlet pipe is mounted tangentially onto the side of the cylindrical part of the cyclone body and the working fluid (gas and particles) is incoming through this section. The exit tube, called the vortex finder, is fixed on the top of the cyclone.

The height, diameter and shape of cyclone, the diameter and inlet geometry of vortex finder can influence considerably the performance of the cyclones. The particle size and the presence of dust collector will also have an effect on the flow characteristics and performance of the cyclone [20].

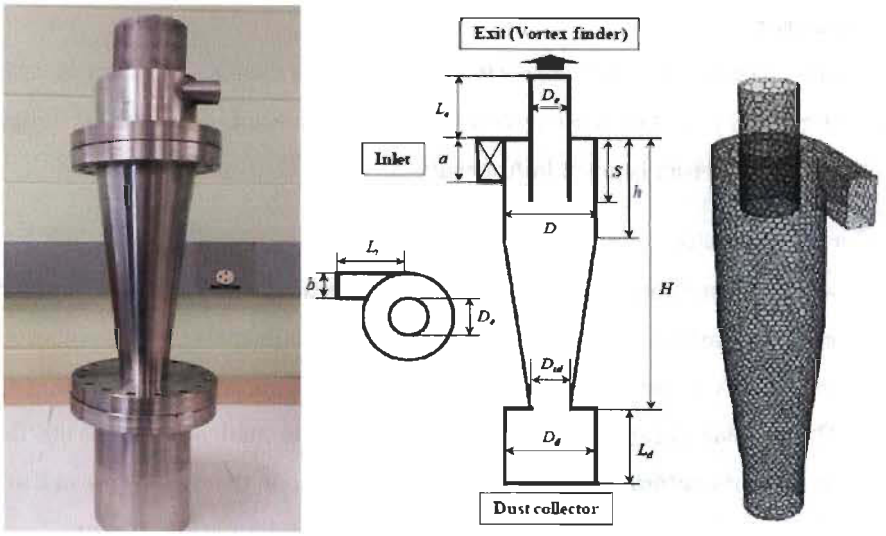

Figure 3.12: Schematics of the cyclone and its grid system.

Table 3.4: Geometrical dimensions for the cyclone.

Dimension	**Value/ D (inch)**
Cyclone diameter (D)	1.0 D (3.14 inch)
Gas outlet diameter (D_e)	0.5 D (3.14 inch)
Dust collector inlet Diameter (D_{id})	0.375D (1.18 inch)
Dust collector Diameter (D_d)	1.0 D (3.14 inch)
Exit length (L_e)	2.0 D (6.29 inch)
Vortex finder length (S)	0.5 D (1.57 inch)
Cylinder length (h)	0.85 D (2.67 inch)
Cyclone length (H)	4.0 D (12.57 inch)
Dust collector length (L_d)	1.7 D (5.35 inch)
Inlet width (a)	0.2 D (0.628 inch)
Inlet height (b)	0.5 D (1.57 inch)
Inlet length (l)	1.0 D (3.14 inch)

4 Results and discussion

4.1 Fluidized reactor

During the experiments, a small amount of nitrogen is used to flush the system to avoid the reaction between biomass and air. The circulating pump is used to increase the flow rate passing through the reactor. The flow rate of the gas can be monitored and controlled by a mass flow controller. The reactor is heated to 573.15-623.15 K by using three mica insulated band heaters. A PID controller along with a solid state relay is used to control the heating rate. A multipoint thermocouple is used to monitor the internal temperature distribution. The pressures at various points of the system are measured by using pressure transducers. All the reactants: cellulose, sodium hydroxide and the catalysts are supported by a distribution plate near the bottom of the reactor and the bottom of the fluidized bed reactor is filled with sufficient water for the reaction to take place, while heating, the water evaporates continuously, the steam reacts with cellulose, sodium hydroxide and nickel catalyst to produce hydrogen gas. The fluid gas is heated by the input heat, flows to the condenser zone where it condenses by the cooling water. The condensed liquid flows back by gravity and capillary effect into the reactor zone. A cyclone separator is provided to capture the fines resulting from particle attrition. A pressure relief valve is installed in the system for 60 psig since the maximum operating pressure for the pump is 75 psig. A filter is placed before the mass flow controller to avoid the entrance of particle to the mass flow controller. The whole system set-up is shown in Figure 4.1.

When the reaction takes place, the reactor is insulated with Al foil backed ceramic insulation fibre to minimize the heat transfer to surroundings by convection. After the temperature and the pressure are stable, the heating is stopped and the Al foil backed ceramic insulation fibre is removed to release the heat to the surrounding environment. The temperature and pressure variation during the heating and cooling process are monitored by Labview to analyse the reaction process.

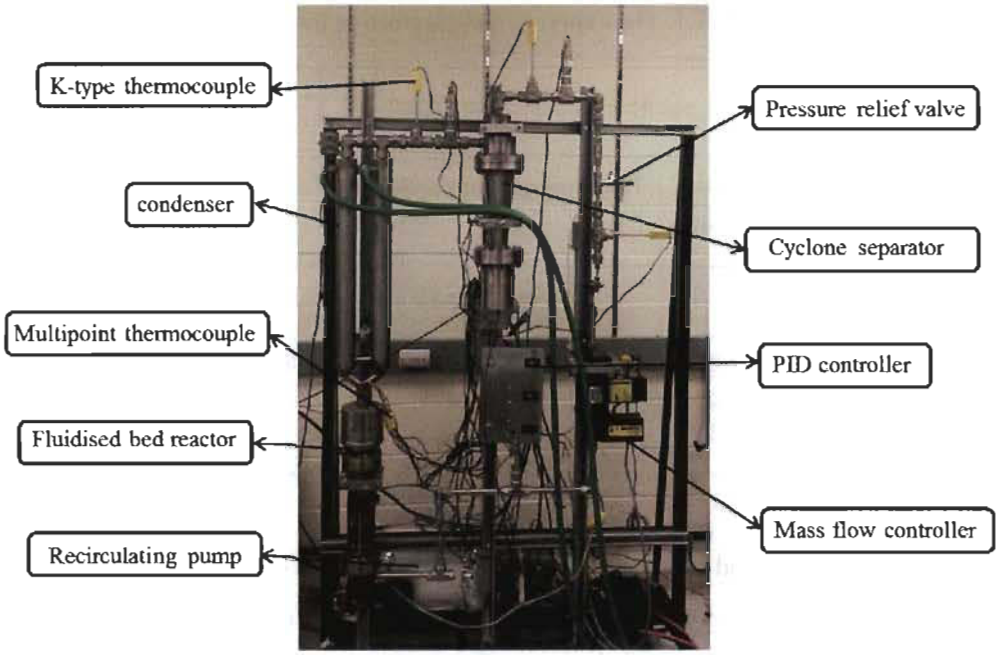

Figure 4.1: The whole system set-up.

4.2 Pre-test

In order to better control the heating process and monitor temperature distribution inside the fluidized reactor by the multipoint thermocouple, a pre-test experiment was conducted without adding the catalyst to observe the reaction phenomenon.

The pre-test run was performed with 1 g of cellulose biomass as feed stock. The experimental parameters are listed in Table 4.1. As per stoichiometry, 1 g of cellulose reacts with 2.97 g of NaOH and excess H_2O (37 mL). 2.97 g of NaOH in 37 mL H_2O constitutes 2 M NaOH solution. 1 g of cellulose, 2.97 g of NaOH were supported by a distribution plate, the bottom of the fluidized bed reactor was filled with 37 mL of H_2O. The reactor was closed air tight, purged with argon at around a pressure of 8 psig which is the initial pressure to make the reactor O_2-free and then heated to different temperatures. The reactor was insulated with Al foil backed ceramic insulation fibre to minimize the heat transfer to surroundings by convection.

Table 4.1: The experimental parameters for pre-test.

Sample runs	Cellulose	NaOH		Pressure (psig) (Ar)			Temperature (K)		
	Mass (g)	Mass (g)	H_2O (mL)	Initial	Maxi	Cool down	Initial	maxi	Cool down
1	1	2.97	37	7.55	19.67	8.25	295.71	473.15	297.81
2	1	2.97	37	7.74	24	8.09	295.06	523.15	298.17
3	1	2.97	37	8.24	25.98	9.97	296.15	663.15	297.01

After the temperature and pressure were stable, the power was switched off, Al foil backed ceramic insulation fibre was removed and the system was allowed to cool down to room temperature. The reactor was cooled to condense the water vapour and hence to exclude the pressure produced from formed water vapour and expanded argon gas. Three heaters (Table 3.2) were used for the reactor and temperature variation inside the reactor during the heating process was clearly observed because of the difference in the heating power and the contact surface area between the reactor and the heaters (Figure 4.2). The temperature distribution inside the reactor was monitored by the multipoint thermocouple.

Figure 4.2: The location of three heaters on the reactor.

The temperature distribution inside the reactor and the pressure-temperature curve were obtained when the reactor was heated to maximum 473.15 K, 523.15 K, 623.15 K and then cooled down to room temperature. The temperature distribution and pressure-temperature curve for the sample heated to maximum 473.15 K are shown in Figure 4.3 a and b, respectively. It can be seen from the temperature varieties that the temperatures change significantly with the different location of the probe point in the multipoint thermocouple, the higher the location of the probe point, the lower the detecting temperature. The temperature distribution is not even in the heating zone. It can be observed that the temperatures fluctuated while heating which indicated the unstable heating process. The maximum pressure was 19.67 psig when reaching the highest temperature and the pressure went down to 8.25 psig when cooling to room temperature. The pressure increase is only 0.7 psig. The reactor was disassembled to check the remaining reactants inside. It can be seen that the cellulose turned to yellow colour and still remained on the distributed plate without reaction.

The unreacted cellulose may imply the low reaction temperature during the heating process, so the heating programme for the PID controller was modified to heat the reactor to higher temperatures (523.15 K and 623.15 K).

For the samples heated to 523.15 K and 623.15 K, the temperature distribution and pressure-temperature curves were shown in Figure 4.3 **c** and **d,** and **e** and **f**, respectively. The temperature gradients for different probe point of multipoint thermocouple still exist as shown in Figure 4.3, in addition, the temperature fluctuation increase with the enhancement of the maximum heating temperature. This is attributed to the increased heating power which causes enlarged difference in the temperature change. With the increase of the maximum heating temperatures, the maximum pressure for the system increased from 24 to 25.98 psig, however, comparing with the initial pressure, the pressure increase can be negligible and the reactants were still remaining in the distribution plate. It is deduced that the reaction is not completed.

Taking the three experiment results into account, the reactants all stayed unreacted. It may be due to the missing water vapor needed for further reaction. During the reaction, the water evaporated, passed through the distribution plate and reacted with cellulose. After the water

evaporated completely, it stayed in the upper part of the reactor, so no more water vapour will participate for further reaction. Our way to solve this problem is by using circulating pump to recirculate the water vapor for further reaction.

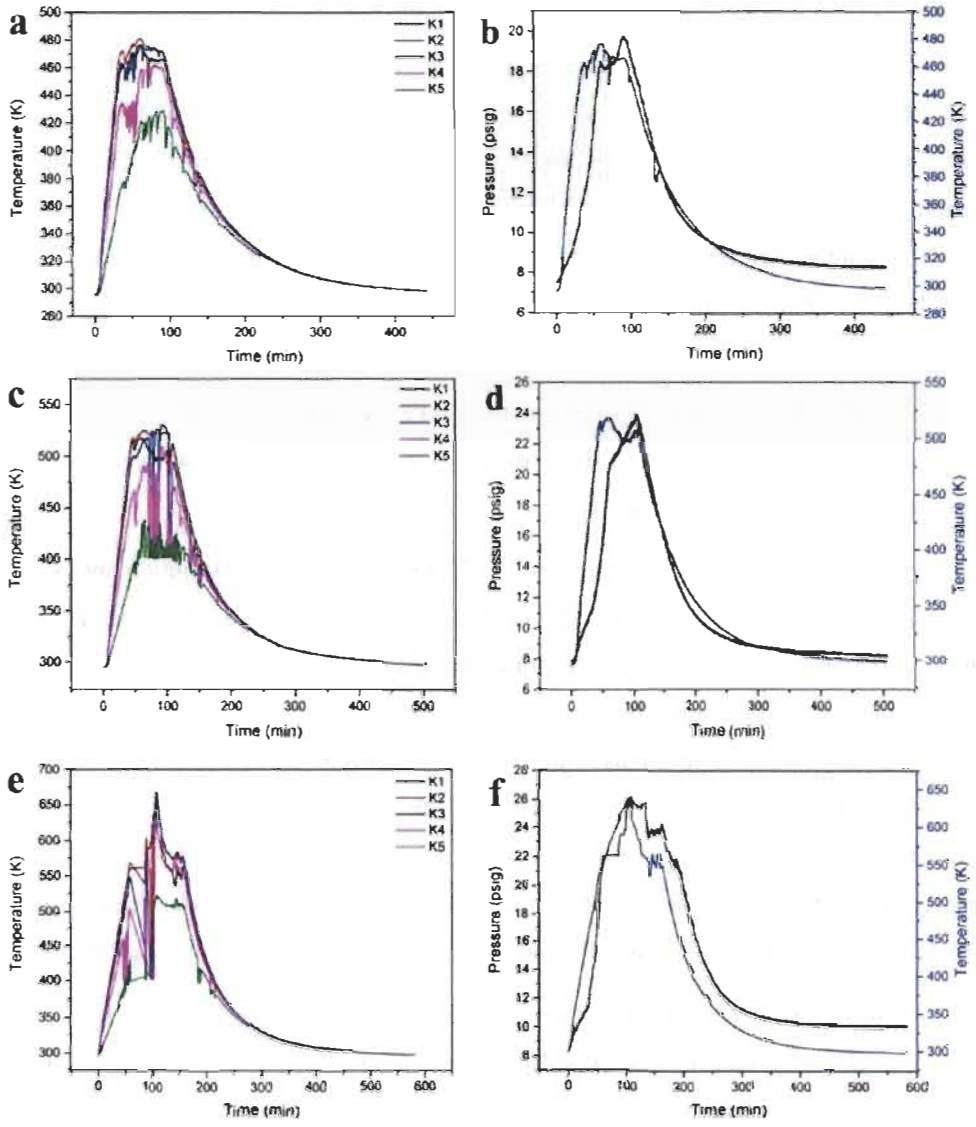

Figure 4.3: The temperature distribution inside the reactor a, c, e and pressure-temperature curve when heated to the maximum temperature: b 473.15 K, d 523.15 K, f 623.15 K.

4.3 Fluidized reactor with circulating pump

Qua-head explosion proof pump is used to circulate the gas inside the system. The inlet of the pump is connected to the three-way valve which is located under the thermocouple and the outlet of the pump is connected to the three-way valve which is located above the mass flow controller (Figure 4.4). The increased flow rate by the pump can be controlled and measured through the mass flow controller.

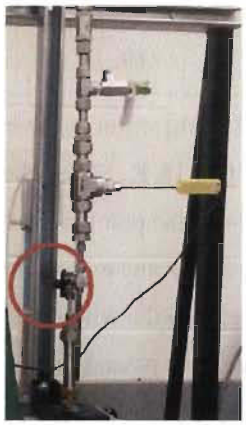

Figure 4.4: The connection of the circulating pump.

The experiments were performed with 1 g of cellulose biomass as feed stock, 2.97 g of NaOH, excess H_2O (37 mL) and 1.5 g nickel-supported alumina balls. 1 g of cellulose, 2.97 g of NaOH and 1.5 g nickel-supported alumina balls were supported by a distribution plate and the bottom of the fluidized bed reactor was filled with 37 mL of H_2O. The reactor was closed air tight.

Table 4.2: The experimental parameters with circulating pump.

	Cellulose	Catalyst	NaOH	Pressure (psig) (Ar)	Temperature (K)	

Sample runs	Mass (g)	Mass (g)	Mass (g)	H_2O (mL)	Initial	Maxi	Cool down	Initial	maxi	Cool down	Flow rate (L/min)
1	1	1.5	2.97	37	12.6	25.4	13.58	295.81	673.15	299.26	60
2	2	1.5	5.92	74	29.0	52.6	21.84	298.09	577.15	294.46	146

Table 4.2: The experimental parameters with circulating pump.

Sample runs	Cellulose	Catalyst	NaOH		Pressure (psig) (Ar)			Temperature (K)			Flow rate (L/min)
	Mass (g)	Mass (g)	Mass (g)	H_2O (mL)	Initial	Maxi	Cool down	Initial	maxi	Cool down	
1	1	1.5	2.97	37	12.6	25.4	13.58	295.81	673.15	299.26	60
2	2	1.5	5.92	74	29.0	52.6	21.84	298.09	577.15	294.46	146

The first run was purged with near 12 psig argon as the initial pressure to make the reactor O_2-free and then heated to maximum 673.15 K. When the temperature went up to 625 K, the pressure was 25.4 psig (Figure 4.5a) and the pump started running with a flow rate of 60 L/min. While the pump was running, the pressure and temperature decreased sharply, it is mainly due to the heat spread in the whole system. In the whole system, only the reactor area was heated by three heaters, so when the heated gas passed from the reactor to the condenser, cyclone separator and pipes, the heat spread to the whole system by convection and heat transfer during the circulating process which brought down the temperature and pressure. After circulating for 1 h, the temperature increased slowly and finally reached the highest temperature at 673.15 K, but the highest pressure went down to around 20 psig (Figure 4.5b). It is due to the evenly distributed pressure and temperature in the whole system. After the system was cooled down to room temperature, the reactor was disassembled to check the remaining reactants. The remaining cellulose was half burned (Figure 4.6) and the pressure increased was only 0.7 psi which indicates that little gas was produced. Considering the pressure and the flow rate of the pump was not high enough to promote the reaction. The second experiment was conducted with higher pressure and flow rate.

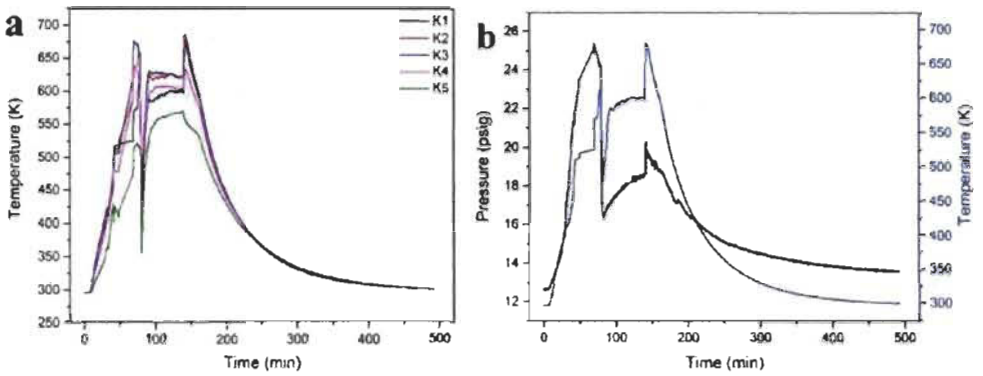

Figure 4.5: (a) Temperature distribution and (b) pressure (black line)-temperature (blue line) curve inside the reactor with circulating pump with the flow rate of 60 L/min.

Figure 4.6: The reactants residue.

Table 4.2: The experimental parameters with circulating pump.

Sample runs	Cellulose	Catalyst	NaOH		Pressure (psig) (Ar)			Temperature (K)			Flow rate (L/min)
	Mass (g)	Mass (g)	Mass (g)	H_2O (mL)	Initial	Maxi	Cool down	Initial	maxi	Cool down	
1	1	1.5	2.97	37	12.6	25.4	13.58	295.81	673.15	299.26	60
2	2	1.5	5.92	74	29.0	52.6	21.84	298.09	577.15	294.46	146

The second run was performed with 2 g of cellulose biomass as feed stock, 5.94 g of NaOH, excess H_2O (74 mL) and 1.5 g nickel-supported alumina balls. 2 g of cellulose, 5.94 g of NaOH and 1.5 g nickel-supported alumina balls were supported by a distribution plate and the bottom of the fluidized bed reactor was filled with 74 mL of H_2O. The reactor was closed air tight, purged with argon and started the pressure at 29 psig. When the temperature reached 577.15 K, the pressure increased to 47.6 psig. While the pump was running with a flow rate of 146 L/min, the temperature inside the reactor suddenly decreased to 393.15 K (Figure 4.7a) because of the heat diffusion. After running the pump for 20 min, there was some abnormal sound from the pump, so this experiment was stopped.

The reactor was disassembled after the system cooled down to room temperature, initially 74 mL of water was used for the reaction, but finally 30 ml of water was collected from the reactor, 20 ml was from the cyclone separator and some water remained inside the tubes. Finally, the pressure decreased 8 psig (Figure 4.7b) which means there were some leakages from the reactor.

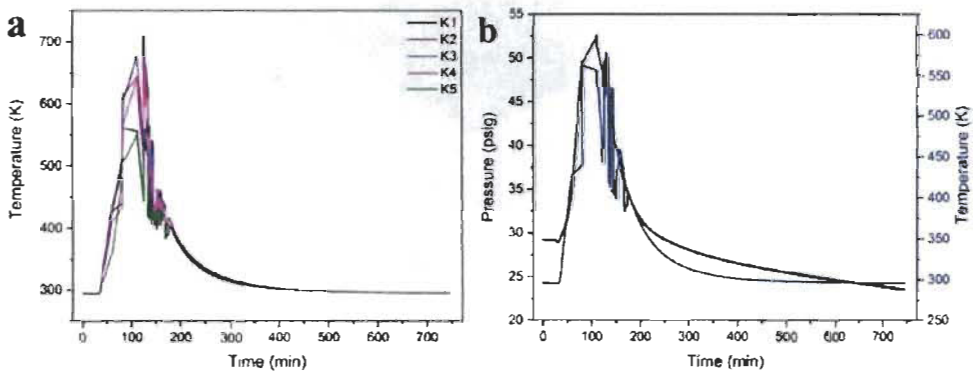

Figure 4.7: (a) Temperature distribution and (b) pressure (black line)-temperature (blue line) curve inside the reactor with circulating pump at the flow rate of 146 L/min.

The unrecovered water was attributed to the cooled moisture remained in the gas. During the circulating process, the gas was initially cooled down by the condenser, but the remaining moisture in the gas further condensed into water drops after passing through the cyclone separator and accumulated on the wall of the pipes. The accumulated water drop may affect the circulating pump, so it is the main reason for the abnormal sound.

In conclusion, when the pump was circulating, the water vapour condensed on the wall of the pipes, so the lost water couldn't participate in the reaction anymore and the reduced gas temperature during circulation is not conducive for the reaction.

4.3.1 Fluidized reactor with modified reactants loading

Aqueous alkaline reforming involves the reaction between water, cellulose and sodium hydroxide. In the fluidized bed reactor, the cellulose was put on the distributor and the produced steam was not enough to promote the reaction, so instead of using water vapor, water was added in the reaction initially.

The reaction was modified to mix all the reactants inside the reactor. Firstly, the sodium hydroxide was dissolved in the water, and then cellulose and catalyst were added to the sodium hydroxide solution until completely dissolved. In this way, the pre-reaction can be promoted during the heating process.

Table 4.3: The experimental parameters for reaction.

Sample runs	Cellulose	Catalyst	NaOH		Pressure (psig) (Ar)			Temperature (K)			Flow rate (L/min)
	Mass (g)	Mass (g)	Mass (g)	H_2O (mL)	Initial	Maxi	Cool down	Initial	maxi	Cool down	
1	1	0.4	2.96	37	20	35.5	24	295.15	445	296.45	N/A
2	3	1.2	8.88	114	20	35	17.9	321.65	623.45	294.55	84
3	3	1.2	8.88	114	10	33	19.24	295.55	623.15	295.47	7

The first experiment was performed for 1 g of cellulose biomass as feed stock, 2.96 g of NaOH, excess H_2O (37 mL) and 0.4 g supported nickel catalyst (~65wt.% on silica/alumina). All the reactants were mixed and loaded to the bottom of the reactor. The reactor was closed air tight, purged with argon. The starting pressure was 20 psig and the maximum heating temperature was 445 K. After heating for 3 h, the power was switched off, Al foil backed ceramic insulation

fibre was removed and the system was allowed to cool down to room temperature. It can be observed that the pressure increased by 4 psig.

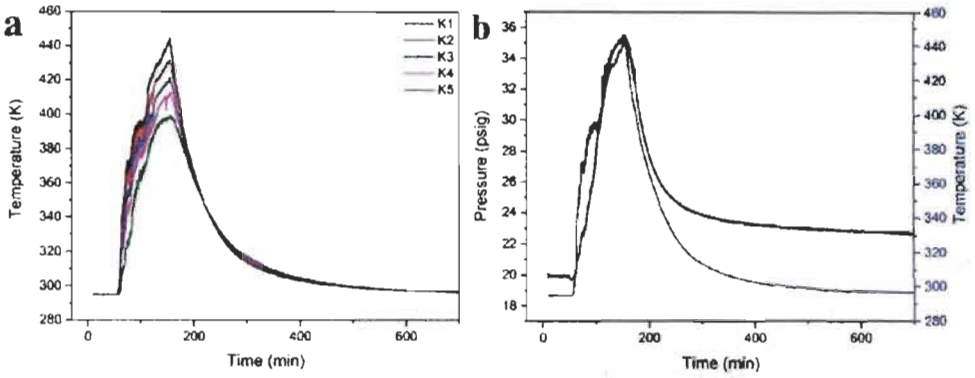

Figure 4.8: (a) Temperatures distribution and (b) pressure (black line)-temperature (blue line) curve inside the reactor.

The gas produced in this experiment was analyzed using the MicroGC and Table 4.4 provides the gas composition data. It was found that hydrogen constitutes about 75% of the gas.

Table 4.4: Gas Chromatography analysis data.

Samples run	MicroGC analysis (Area %)			
	H_2	O_2	N_2	CH_4
1	75	7.57	15.77	1.59
2	80	0.93	1.42	0.28
3	97.26	0.20	0.25	0.82

In this run, the temperature was not high enough, so the second run was performed with higher temperature and circulating pump.

The second run was performed with 3 g cellulose 8.88 g NaOH 111 mL H_2O and 1.2 g catalyst. The system was purged with argon at 20 psig. While heating, the pump was running at the same time. Initially, the flow rate was 64 L/min, after pumping for 30 min, the flow rate increased to 84 L/min, the pressure increased to 35 psig. After reaching the highest temperature,

the temperature inside the reactor decreased to 400 K sharply and the pressure also decreased gradually. When the system was cooled down to room temperature, the pressure decreased to 17.9 psig, which implied the leakage of the system (Figure 4.9). The sudden decrease of the temperature and the slightly decreased pressure also implied the leakage of the system.

The produced gas was analyzed using MicroGC. It was found that hydrogen constitutes about 80% of the gas (Table 4.4).

After the gas was analysed, the system was disassembled, there was no water remaining in the cyclone and some cellulose was pushed by the pump and stayed in the gasket without reaction.

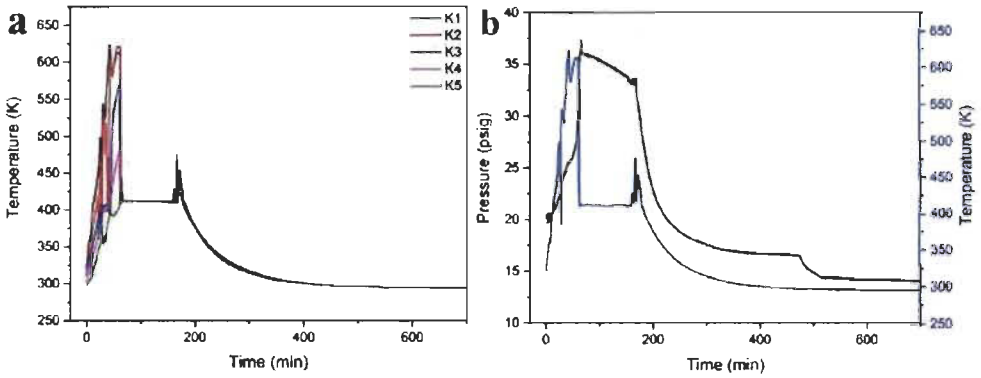

Figure 4.9: (a) Temperatures distribution and (b) pressure (black line)-temperature (blue line) curve inside the reactor with circulating pump at the flow rate of 84 L/min.

As some of the reactants were pushed by the pump to the gasket, the flow rate of the pump was decreased in the third run. 3 g cellulose, 8.88 g NaOH, 111 mL H_2O and 1.2 g supported nickel catalyst were used as reactants. The system was purged with argon at 10 psig and heated to 623.15 K within 1 h and kept for 2 h. In the meantime, the pump was running at the flow rate of 7 L/min for 3 h. The maximum pressure was 33 psig. The cooling down pressure was 19.24 psig which indicated 9.24 psig increase of the pressure (Figure 4.10b).

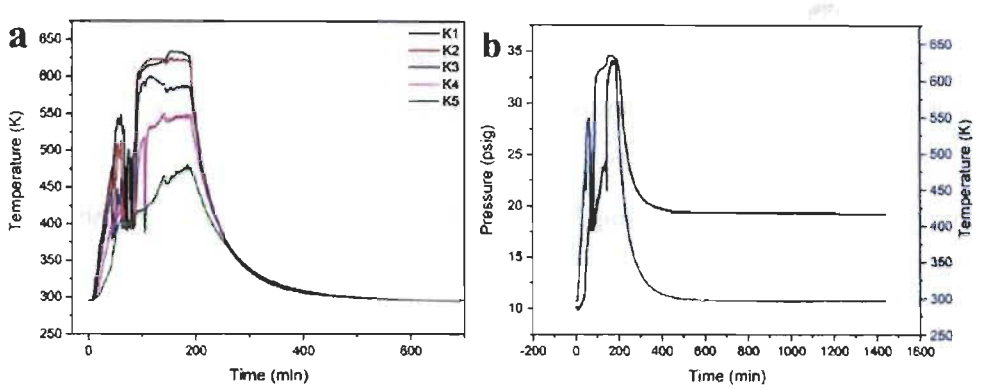

Figure 4.10: (a) Temperatures distribution and (b) pressure (black line)-temperature (blue line) curve inside the reactor with circulating pump at the flow rate of 7 L/min.

The produced gas was analyzed using MicroGC and the hydrogen constitutes about 97.26% of the gas (Table 4.4).

After the gas was analysed, the system was disassembled. There was no water remaining in the reactor. We collected 100 mL H_2O from cyclone separator and some water was accumulated inside the tubes which indicated the loss of water during the reaction.

4.3.1.1 Hydrogen mass and efficiency calculation

In order to calculate the hydrogen production efficiency, the third run is taken as an example. The GC analysis shows that hydrogen constitutes 97.26 % of the total gas produced and the pressure after cooling down the reactor is 19.24 psig. The mass of hydrogen produced is calculated using real gas equation

$$PV = ZnRT$$

Where P is the final pressure after cooling down the reactor, V is the volume of the reactor, Z is the compressibility factor, n is the number of moles of gas, R is the universal gas constant (8.314 J mol^{-1} K^{-1}) and T is the final cool down temperature. The calculation is based on the number of moles of gas present before and after the experiment run.

The number of moles of argon, n_1 is calculated based on the initial pressure (10 psig), reactor volume (0.0042 m^3) and initial temperature (295.55 K) using the real gas equation. The value of the compressibility factor (Z) is obtained from the NIST table at temperature (295.55 K) and pressure 10 psig (69981.79 Pa). The total number of moles (n_1+n_2) after cooling is calculated based on the final cool down pressure (19.24 psig), where n_2 denotes the number of moles of H_2. The value of the compressibility factor (Z) is obtained from NIST table based on the mole fractions of H_2 and argon calculated from the partial pressures. Based on the final cool down pressure, reactor volume and cool down temperature, the number of moles of hydrogen produced is found to be 0.1043 moles, which constitutes 0.2086 g. The mass of H_2 supposed to be obtained from 3 g of cellulose with 100% conversion is 0.444 g. Hence the efficiency of the process is given as:

$$\eta = \frac{\text{Mass of H2 produced from 3g cellulose}}{\text{Mass of H2 present from 3g cellulose}}$$

The efficiency of the process is found to be 46.98 % from the production of 0.2086 g of H_2 from 3 g of cellulose. The drop in efficiency is due to the loss of water which affects the hydrogen production rate.

4.3.2 Modified fluidized reactor

In order to reuse the condensed water, the system was modified as is shown in Figure 4.11. A ¼ inch Swagelok tube was used to connect the cyclone separator with the tube which was attached to the bottom of the reactor. The condensed water in the cyclone separator will go back to the reactor by gravity and the flow rate of the pump.

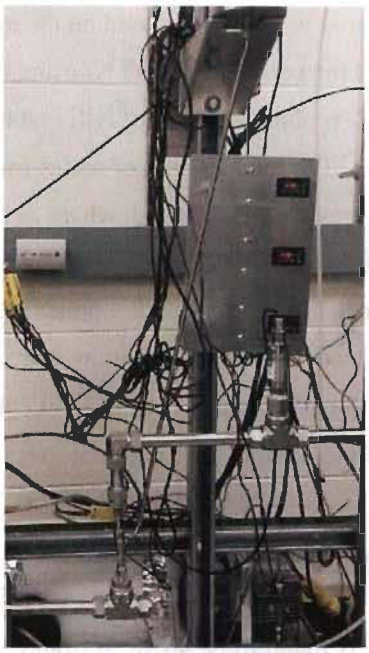

Figure 4.11: The modified set-up.

In the modified system, 2 g cellulose, 5.92 g NaOH, 74 mL H_2O and 0.8 g supported nickel catalyst (~65wt.% on silica/alumina) were used as reactants (Table 4.5). The starting pressure is about 14.5 psig. All the reactants were mixed together at the bottom of the reactor until the cellulose was completely dissolved in the sodium hydroxide solution. In order to evenly mix the reactants during the reaction, a bended tube was inserted to the bottom of the reactor. While circulating, the flowing gas will generate the bubbles inside the solution. After heating for 3 h, the power was switched off, Al foil backed ceramic insulation fibre was removed and the system was allowed to cool down to room temperature. It can be observed that the pressure increased 4 psig (Figure 4.12).

There were some smokes from the pump after running for 3 hours. The pump was opened and checked, it can be observed that some water is remaining inside the pump which is due to the condensed water steam.

Table 4.5: The experimental parameters for modified reactor.

Cellulose	Catalyst	NaOH		Pressure (psig) (Ar)			Temperature (K)			Flow rate (L/min)
Mass (g)	Mass (g)	Mass (g)	H_2O (mL)	Initial	Maxi	Cool down	Initial	maxi	Cool down	
2	0.8	5.92	74	14.5	33.66	18.4	295.15	705.25	300.15	7

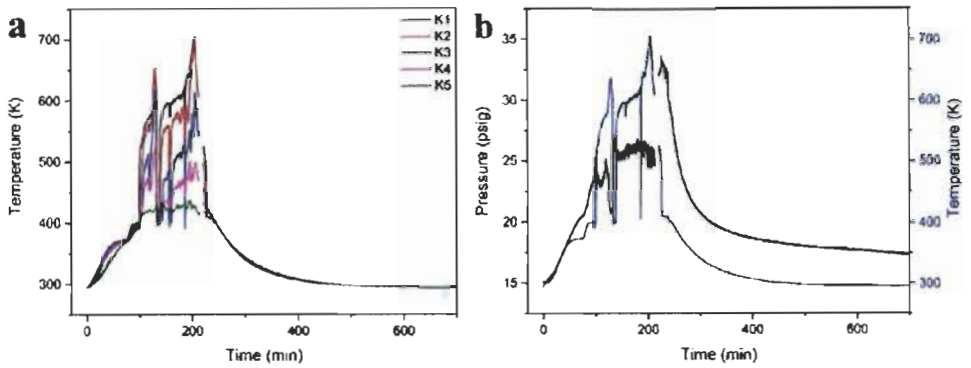

Figure 4.12: (a) Temperatures distribution and (b) pressure (black line)-temperature (blue line) curve for the modified reactor.

The produced gas was analyzed using MicroGC and the hydrogen constitutes about 94% of the gas.

The hydrogen production efficiency is calculated based on the number of moles of gas present before and after the experiment run which is mentioned in Section 4.3.1.1. The number of moles of argon, n_1 is calculated based on the initial pressure (14.5 psig), reactor volume (0.0042 m^3) and initial temperature (295.15 K) using the real gas equation. The value of the compressibility factor (Z) is obtained from the NIST table at temperature (295.15 K) and pressure 14.5 psig (99973 Pa).The total number of moles (n_1+n_2) after cooling is calculated based on the final cool down pressure (18.4 psig), where n_2 denotes the number of moles of H_2. The value of the compressibility factor (Z) is obtained from NIST table based on the mole fractions of H_2 and argon calculated from the partial pressures. Based on the final cool down pressure, reactor volume and cool down temperature, the number of moles of hydrogen

produced is found to be 0.04 moles, which constitutes 0.08 g. The mass of H_2 supposed to be obtained from 2 g of cellulose with 100% conversion is 0.296 g. Hence the efficiency of the process is given as:

$$\eta = \frac{\text{Mass of } H_2 \text{ produced from 3g cellulose}}{\text{Mass of } H_2 \text{ present from 3g cellulose}}$$

The efficiency of the process is found to be 25.4 % from the production of 0.296 g of H_2 from 2 g of cellulose. The drop in efficiency is due to the condensed water which affects the hydrogen production rate.

Even the system was modified to reuse the condensed water; it did not work as expected. The hydrogen production efficiency is not high, so the further modification was made.

4.4 Batch reactor

Figure 4.13: The bath reactor.

This system was modified as shown in Figure 4.13. The condenser, cyclone separator and mass flow controller were removed, only the reactor and heaters were kept. Before, the same experiment was conducted in another bath reactor, compared with the previous designed reactor, this batch reactor can provide easier loading of reactants.

Table 4.6: The experimental parameters for batch reactor.

Sample runs	Cellulose	Catalyst	NaOH		Pressure (psig) (Ar)			Temperature (K)		
	Mass (g)	Mass (g)	Mass (g)	H_2O (mL)	Initial	Maxi	Cool down	Initial	maxi	Cool down
1	1	0.4	2.96	37	20.38	325.26	25.78	293.58	627.07	301.42
2	1	1.5	2.96	37	20.56	107.48	25.71	294.76	583.69	296.34

1 g cellulose, 2.96 g NaOH, 37 mL H_2O and 0.4 g supported nickel catalyst (~65wt.% on silica/alumina) were used as reactants. All the reactants were mixed inside the reactor and the starting pressure is about 20.38 psig. The pressure-temperature curve is shown in Figure 4.14.

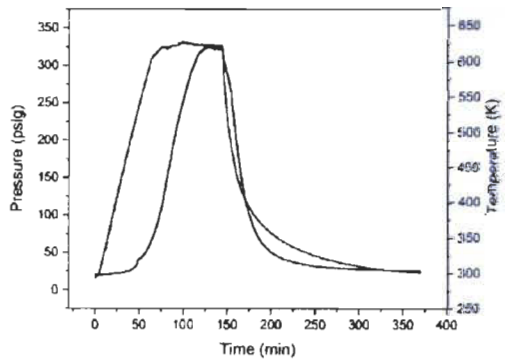

Figure 4.14: pressure (black line)-temperature (blue line) curve for the batch reactor.

The produced gas was analyzed using MicroGC and the hydrogen constitutes about 97% of the gas.

The hydrogen production efficiency is calculated based on the number of moles of gas present before and after the experiment run which is mentioned in Section 4.3.1.1. The number of moles of argon, n_1 is calculated based on the initial pressure (20.38 psig), reactor volume (0.001186 m^3) and initial temperature (293.58 K) using the real gas equation. The value of the compressibility factor (Z) is obtained from the NIST table at temperature (293.58 K) and pressure 20.38 psig (140515.15 Pa).The total number of moles (n_1+n_2) after cooling is

calculated based on the final pressure (25.78 psig) after the system cooled down, where n_2 denotes the number of moles of H_2. The value of the compressibility factor (Z) is obtained from NIST table based on the mole fractions of H_2 and argon calculated from the partial pressures. Based on the final cool down pressure, reactor volume and cool down temperature, the number of moles of hydrogen produced is found to be 0.016 moles, which constitutes 0.032 g. The mass of H_2 supposed to be obtained from 1 g of cellulose with 100% conversion is 0.148 g. Hence the efficiency of the process is given as:

$$\eta = \frac{\text{Mass of } H_2 \text{ produced from 1g cellulose}}{\text{Mass of } H_2 \text{ present from 1g cellulose}}$$

The efficiency of the process is found to be 20.97 % from the production of 0.032 g of H_2 from 1 g of cellulose. The efficiency for the reaction is low, in order to improve the efficiency, the synthesized catalyst Ni/Al_2O_3-B was used in the reaction instead of supported nickel catalyst.

1 g cellulose, 2.96 g NaOH, 37 mL H_2O and 1.5 g Ni/Al_2O_3-B were used as reactants. All the reactants were mixed inside the reactor and the starting pressure is about 20.56 psig. The produced gas was analyzed using MicroGC and the hydrogen constitutes about 98% of the gas.

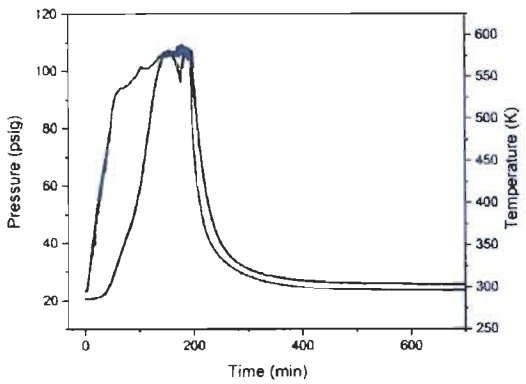

Figure 4.15: pressure (black line)-temperature (blue line) curve for the batch reactor with Ni/Al_2O_3-B catalyst.

The hydrogen production efficiency is calculated based on the number of moles of gas present before and after the experiment run which is mentioned in Section 4.3.1.1. The number of moles of argon, n_1 is calculated based on the initial pressure (20.56 psig), reactor volume

(0.001186 m^3) and initial temperature (294.76 K) using the real gas equation. The value of the compressibility factor (Z) is obtained from the NIST table at temperature (294.76 K) and pressure 20.56 psig (141756.21Pa).The total number of moles (n_1+n_2) after cooling is calculated based on the final cool down pressure (25.71 psig), where n_2 denotes the number of moles of H_2. The value of the compressibility factor (Z) is obtained from NIST table based on the mole fractions of H_2 and argon calculated from the partial pressures. Based on the final cool down pressure, reactor volume and cool down temperature, the number of moles of hydrogen produced is found to be 0.0167 moles, which constitutes 0.033 g. The mass of H_2 supposed to be obtained from 1 g of cellulose with 100% conversion is 0.148 g. Hence the efficiency of the process is given as:

$$\eta = \frac{\text{Mass of } H_2 \text{ produced from 1g cellulose}}{\text{Mass of } H_2 \text{ present from 1g cellulose}}$$

The efficiency of the process is found to be 22.15% from the production of 0.032 g of H_2 from 1 g of cellulose.

The hydrogen production efficiency did not increase after the catalyst was changed. Compared with the previous batch reactor, this modified reactor is not efficient enough to improve the hydrogen production. This may attribute to the inefficient heating. In the modified reactor, the three heats was distributed separator which cause the temperature gradient inside the reactor.

The leaks occurred at the bottom of the reactor were a persistent problem, the gasket between the lower and upper part of the reactor should be tightened by screws each time. The unevenly tight may cause leaks in high temperature.

5 Conclusion

The aqueous alkaline reforming was conducted in the designed fluidized reactor system, which consists of fluidized bed reactor, condenser, cyclone separator, mass flow controller and pump.

Instead of the solid and gas reactants for the widely used fluidized reactor, water is included in our system to initially dissolve all the reactants for further reaction. The circulating pump circulates the gas to enlarge the contact surface area between the cellulose and water vapor, but the disadvantage is more obvious. While circulating, the heated gas passed from the heating zone to the condenser, cyclone separator and pipes, the heat spread to the whole system by convection and heat transfer during the circulating process which brought down the temperature and pressures and generated the temperature gradients inside the reactor as well, furthermore, the loss of water during circulating because of the condensed water vapour accumulated on the wall of pipes and inside the pump is another aspect which decrease the hydrogen production efficiency.

When the experiment was conducted with 3 g cellulose, 8.88 g NaOH, 111 mL H_2O and 1.2 g supported nickel catalyst with the flow rate of 7 L/min, the hydrogen production efficiency was highest at 46.98 % which constitute 97.26 % hydrogen. It is similar to the hydrogen production efficiency in the previous batch reactor.

The fluidized reactor was also modified as a batch reactor, but the different heating capacity of three heaters generates temperature gradients inside the reactor which cause the low hydrogen production efficiency.

The hydrogen production for aqueous alkaline reforming in fluidized reactor can be further investigated in a small scale of set-up which provide evenly heating and adjustable flow rate in high temperature to avoid the condensed water for the system.

6 References

[1] R.D. Cortright, R.R. Davda, J.A. Dumesic, Hydrogen from catalytic reforming of biomass-derived hydrocarbons in liquid water, Nature, 418 (2002) 964-967.

[2] H. Balat, E. Kırtay, Hydrogen from biomass – Present scenario and future prospects, International Journal of Hydrogen Energy, 35 (2010) 7416-7426.

[3] D.B. Levin, R. Chahine, Challenges for renewable hydrogen production from biomass, International Journal of Hydrogen Energy, 35 (2010) 4962-4969.

[4] G.W. Huber, S. Iborra, A. Corma, Synthesis of transportation fuels from biomass: Chemistry, catalysts, and engineering, Chemical Reviews, 106 (2006) 4044-4098.

[5] M. Ni, D.Y.C. Leung, M.K.H. Leung, K. Sumathy, An overview of hydrogen production from biomass, Fuel Processing Technology, 87 (2006) 461-472.

[6] A. Tanksale, J.N. Beltramini, G.M. Lu, A review of catalytic hydrogen production processes from biomass, Renewable and Sustainable Energy Reviews, 14 (2010) 166-182.

[7] J.D. Holladay, J. Hu, D.L. King, Y. Wang, An overview of hydrogen production technologies, Catalysis Today, 139 (2009) 244-260.

[8] J. Turner, G. Sverdrup, M.K. Mann, P.-C. Maness, B. Kroposki, M. Ghirardi, R.J. Evans, D. Blake, Renewable hydrogen production, International Journal of Energy Research, 32 (2008) 379-407.

[9] P. McKendry, Energy production from biomass (part 2): conversion technologies, Bioresource Technology, 83 (2002) 47-54.

[10] A.V. Bridgwater, Renewable fuels and chemicals by thermal processing of biomass, Chemical Engineering Journal, 91 (2003) 87-102.

[11] A. Gómez-Barea, B. Leckner, Modeling of biomass gasification in fluidized bed, Progress in Energy and Combustion Science, 36 (2010) 444-509.

[12] D. Sutton, B. Kelleher, J.R.H. Ross, Review of literature on catalysts for biomass gasification, Fuel Processing Technology, 73 (2001) 155-173.

[13] Ž. Knez, E. Markočič, M.K. Hrnčič, M. Ravber, M. Škerget, High pressure water reforming of biomass for energy and chemicals: A short review, The Journal of Supercritical Fluids, 96 (2015) 46-52.

[14] S.K. Saxena, Hydrogen production by chemically reacting species, International Journal of Hydrogen Energy, 28 (2003) 49-53.

[15] M. Ishida, K. Otsuka, S. Takenaka, I. Yamanaka, One-step production of CO- and CO2-free hydrogen from biomass, Journal of Chemical Technology & Biotechnology, 80 (2005) 281-284.

[16] M. Ishida, S. Takenaka, I. Yamanaka, K. Otsuka, Production of COx-Free Hydrogen from Biomass and NaOH Mixture: Effect of Catalysts, Energy & Fuels, 20 (2006) 748-753.

[17] B. Reichman, W. Mays, J. Strebe, M. Fetcenko, Ovonic Renewable Hydrogen (ORH) – low temperature hydrogen from renewable fuels, International Journal of Hydrogen Energy, 35 (2010) 4918-4924.

[18] D. Kunii, O. Levenspiel, Fluidization engineering, Elsevier2013.

[19] J. Holman, Heat transfer, Eighth SI Metric Edition, McGraw-Hill Inc, 2001.

[20] The effect of cyclone shape and dust collector on gas-solid flow and performance.

Appendix A

Ψ is the sphericity, which is a measure of a particle's nonideality in both shape and roughness. It is calculated by visualizing a sphere whose volume is equal to the particle's, and dividing the surface area of this sphere by the actually measured surface area of the particle, we use balls as catalyst, so the sphericity of the ball is 1.

$$\Psi = 1$$

ε_{mf} is the void fraction at the point of minimum fluidization. It appears in many of the equations describing fluidized bed characteristics. There is a correlation that apparently gives quite accurate predictions of measured values of ε_{mf} when the particles in the fluidized bed.

$$\varepsilon_{mf} = (0.071/\Psi)^{1/3} = 0.414$$

The gravity term is calculated as:

$$\eta = g(\rho_c - \rho_g) = 980\ \text{cm/s}^2 \times (1.5 - 1.7 \times 10^{-3})\text{g/cm}^3 = 1468\ \text{g/cm}^2\text{s}^2$$

The minimum fluidization velocity is:

$$u_{mf} = \frac{(\Psi d_p)^2}{150\mu}\eta\frac{\varepsilon_{mf}^3}{1-\varepsilon_{mf}} = \frac{(1\times0.1)^2}{150\times3.79\times10^{-4}} \times 1468 \times \frac{0.414^3}{1-0.414} = 31.26\ \text{cm/s} = 0.3\ \text{m/s}$$

When the upward velocity of the gas exceeds the free-fall terminal velocity of the particle, u_t, the particle will be carried upward with the gas stream. For fine particles, the Reynolds numbers will be small, and two relationships presented by Kunii and Levenspiel [12] are:

$$u_t = \eta d_p^2 / 18\mu \qquad Re < 0.4$$

$$u_t = \left(1.78 \times 10^{-2}\ \eta^2/\rho_g\mu\right)^{1/3}(d_p) \qquad (0.4 < Re < 500)$$

Reynolds number:

$$R_e = \frac{\rho_g v d_p}{\mu} = \frac{1.7 \times 10^{-3} \times 31.26 \times 0.1}{3.79 \times 10^{-4}} = 14.02$$

The maximum fluidization:

$$u_t = \left(\frac{1.78 \times 10^{-2}\eta^2}{\rho_g \mu}\right)^{\frac{1}{3}} (d_p) \qquad 0.4 < R_e < 500$$

$$u_t = \left(\frac{1.78 \times 10^{-2}\eta^2}{\rho_g \mu}\right)^{\frac{1}{3}} (d_p) = \left(\frac{1.78 \times 10^{-2} \times 1468^2}{3.79 \times 10^{-4} \times 1.7 \times 10^{-3}}\right)^{\frac{1}{3}} (0.1) = 3.90 \text{ m/s}$$

Q_m: Minimum flow rate

$$Q_m = \text{A}\, u_m = \frac{\pi D^2}{4} u = \frac{3.14 \times 0.0508^2}{4} \times 0.3 = 6.077 \times 10^{-4}\, \text{m}^3/\text{s} = 36\, \text{L/min}$$

Q_t: Maximum flow rate

$$Q_t = \text{A}\, u_t = \frac{\pi D^2}{4} u = \frac{3.14 \times 0.0508^2}{4} \times 3.9 = 7.9 \times 10^{-3}\, \text{m}^3/\text{s} == 474\, \text{L/min}$$

The calculation above is based on the catalyst size and density, if we change the size or/and the density of the catalyst, the minimum and maximum fluidization velocity are listed in Table A1. The pump was chosen according to the minimum fluidization velocity.

Table A1: The minimum and maximum flow rate according to different catalyst.

Diameter of catalyst (cm)	Density of catalyst (g/cm^3)	Density of gas (g/cm^3)	Minimum fluidization velocity (m/s)	Maximum fluidization velocity (m/s)	Minimum flow rate (L/min)	Maximum flow rate (L/min)
0.25	0.50	0.0017	0.65	4.69	78.96	569.66
0.20	0.50	0.0017	0.42	3.75	50.53	455.73
0.15	0.50	0.0017	0.23	2.81	28.43	341.80
0.10	0.50	0.0017	0.10	1.87	12.63	227.86
0.25	1.00	0.0017	1.30	7.45	158.19	905.31
0.20	1.00	0.0017	0.83	5.96	101.24	724.25
0.15	1.00	0.0017	0.47	4.47	56.95	543.19
0.10	1.00	0.0017	0.21	2.98	25.31	362.12
0.20	1.50	0.0017	1.25	7.81	151.95	949.39
0.15	1.50	0.0017	0.70	5.86	85.47	712.04
0.10	1.50	0.0017	0.31	3.91	37.99	474.70
0.15	0.80	0.0017	0.37	3.85	45.54	467.97

Appendix B

Argon is used as inert gas to purge the system before heating the reactor in order to remove the air from the reactor to avoid other chemical reactions. During the circulating process, argon gas is the fluid passing through the pipe. The temperature and pressure of argon gas entering the pipe (T_{in}) are 573.15 K and 14.7 psig, respectively. Assuming the temperature of the gas passing out of the pipe (T_{out}) is 353.15 K. The parameters of the argon gas are shown in **Erreur ! Source du renvoi introuvable.**.

Table B1: The parameters of the argon flowing through the inner pipe of the condenser.

Symbol	Characterisation		Unit
ρ_p	mass density	0.84	kg/m^3
μ_p	viscosity	3.79×10^{-5}	kg/m/s
C_P	specific heat	520.33	J/kg K
K_P	thermal conductivity	26.8×10^{-3}	W/m/K
M	mass flow rate	5.93×10^{-4}	kg/s

The inside and outside diameter of the inner pipe are 0.0212 m (d_i) and 0.0254 m (d_o) respectively. The inside and outside diameter of the outer pipe are 0.042 m (D_i) and 0.0508 m (D_o) respectively.

The mass flow rate of the argon gas is m_p :

$$m_p = \rho_p \times \pi \times \frac{{d_i}^2}{4} \times v = 0.84 \times 3.14 \times \frac{0.0212^2}{4} \times 2 = 5.93 \times 10^{-4}\ \text{kg/s}$$

The heat transfer coefficient of the inner pipe is h_i

$$h_i = \frac{Am_p{}^{0.8}}{d^{1.8}}$$

$$A=0.032756K_P\left(\frac{1}{\mu_p}\right)^{0.8}\left(\frac{C_P\mu_P}{K_P}\right)^{\frac{1}{3}}$$

$$= 0.032756 \times 26.8 \times 10^{-3}\left(\frac{1}{3.79\times10^{-5}}\right)^{0.8}\left(\frac{520.33\times3.79\times10^{-5}}{26.8\times10^{-3}}\right)^{\frac{1}{3}}$$

$$= 2.73$$

$$h_i = \frac{2.73 \times m^{0.8}}{d_i{}^{1.8}} = \frac{2.73 \times (5.93 \times 10^{-4})^{0.8}}{0.0212^{1.8}} = 7.37\ W/\mathrm{m}^2\mathrm{K}$$

On a unit-length basis the thermal resistance on the inside is

$$R_i = \frac{1}{h_i A_i} = \frac{1}{h_i 2\pi r_i} = \frac{1}{7.37 \times 2 \times 3.14 \times 0.0106} = 2.04$$

Table B2: The parameters of the water flowing in the annulus.

Symbol	Characterisation		Unit
ρ_a	mass density	1000	kg/m^3
μ_a	viscosity	1×10^{-3}	kg/m/s
C_a	specific heat	4.18×10^3	J/kg K
K_a	thermal conductivity	0.6	W/m/K
m_a	mass flow rate	0.087	kg/s

The inlet temperature of the water flowing through the annulus is t_{in}, the pressure of the water flowing through the annulus is 14.7 psig.

$$t_{in} = 293.15\ \mathrm{K}$$

$$P = 1\mathrm{atm} = 14.7\ \mathrm{psig}$$

The mass flow rate of the water is measured according to the maximum flow rate of the tape water, the parameters of the water flowing in the annulus is given in Table B2:

$$m_a = 87\frac{\text{ml}}{\text{s}} = 87\text{g/s} = 0.087\ \text{kg/s}$$

$$D = 2\ \text{inches} = 0.0508\ \text{m}$$

The heat transfer coefficient of the annulus is h_o :

$$h_o = \frac{Bd^{0.2}}{x}$$

$$x = D^2 - d^2 = 0.042^2 - 0.0212^2 = 1.31 \times 10^{-3}\ \text{m}^2$$

$$\text{B}=0.032756K_a \left(\frac{m_a}{\mu_a}\right)^{0.8} \left(\frac{C_a\mu_a}{K_a}\right)^{\frac{1}{3}}$$

$$=0.032756\times 0.6 \times \left(\frac{0.087}{1\times10^{-3}}\right)^{0.8} \left(\frac{4.18\times10^3\times1\times10^{-3}}{0.6}\right)^{\frac{1}{3}}$$

$$=1.34$$

$$h_o = \frac{Bd^{0.2}}{x} = \frac{1.34\times0.0254^{0.2}}{1.31\times10^{-3}} = 490\ \text{J/m}^2\ \text{s K}$$

On a unit-length basis the thermal resistance on the annulus is

$$R_o = \frac{1}{h_o A_o} = \frac{1}{h_o 2\pi r_o} = \frac{1}{490 \times 2 \times 3.14 \times 0.0127} = 0.026$$

Outside radius of the inner tube is r_o

Inside radius of the inner tube is r_i

$$r_o = 0.0127\ \text{m}$$

$$r_i = 0.0106\ \text{m}$$

The condenser is made of stainless steel, the thermal conductivity of the stainless steel is

K = 19 W/ m·K

For unit length of the pipe the thermal resistance of the stainless steel is

$$R_S = \frac{In(r_o/r_i)}{2\pi k} = \frac{In(0.0127/0.0106)}{2\times3.14\times19} = 1.52 \times 10^{-3}$$

The calculation illustrates that the thermal heat transfer inside controls the overall heat-transfer because the R_i is larger than R_o and R_s. The overall heater transfer coefficient is based on the inside area of the inner pipe.

$$U = \frac{1}{A_i(R_i+R_S+R_o)} = \frac{1}{2\pi r_i(R_i+R_S+R_o)} = \frac{1}{2\times3.14\times0.0106\times(2.16+1.52\times10^{-3}+0.026)} = 6.82\ \mathrm{J/m^2\ s\ K}$$

$U = 6.82\ \mathrm{J/m^2\ s\ K}$

The total heat transfer is determined from the energy absorbed by the argon gas:

$q = m_p C_P \Delta T_p$

$= 8.5 \times 10^{-4} \times 520.33 \times 220$

$=97$ J/s

The heat released by the argon gas is absorbed by the water. The outlet temperature of the water flowing through the annulus is t_{out}.

$q = m_a C_a \Delta T_a = 0.087 \times 4180 \Delta T_a$

$\Delta T_a = 0.27\mathrm{K}$

$t_{out} = 293.42\ \mathrm{K}$

Since all the fluid temperatures are known, in the counter flow, the LMTD can be calculated by using the temperature scheme [7]:

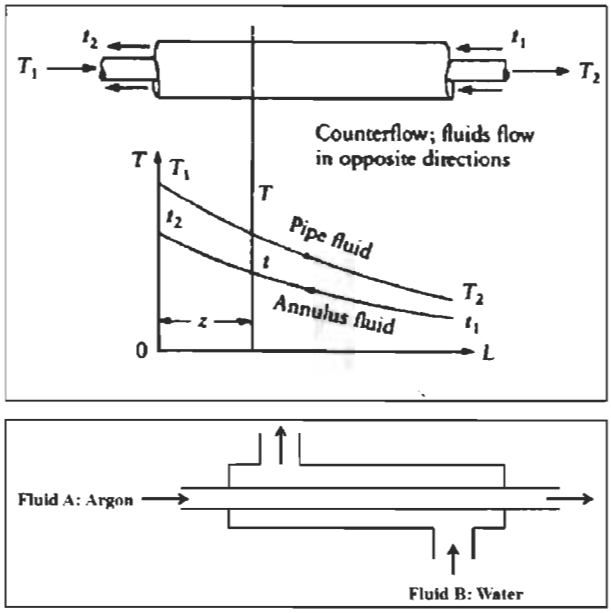

Figure B1: Temperature profile for counter flow in double-pipe heat exchanger.

$$\Delta T_m = \frac{(T_{in} - t_{in}) - (T_{out} - t_{out})}{ln[(T_{in} - t_{in})/(T_{out} - t_{out})]} = \frac{(573.15 - 293.15) - (353.15 - 293.42)}{ln[(573.15 - 293.15)/(353.15 - 293.42)]}$$
$$= 142.6$$

The total flow rate area is:

$$A = \frac{q}{U\Delta T_m} = \frac{97}{6.82 \times 142.6} = 0.1 \text{ m}^2$$

The length of tube for this type of exchanger is:

$$L = \frac{A}{\pi d} = \frac{0.1}{3.14 \times 0.0254} = 1.25 \text{ m} = 49.2 \text{ inches}$$

This length is greater than the practical application length, so we must use more than one tube pass. Considering the actual application, we used two tube passes as shown in **Erreur ! Source du renvoi introuvable.**. The length of each inner pipe is 25 inches, the inside and outside diameter of the inner pipe are 0.0212 m and 0.0254 m respectively. The inside and outside diameter of the outer pipe are 0.042 m and 0.0508 m, respectively.

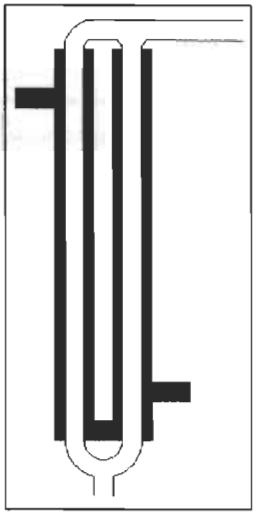

Figure B2: The design of the heat exchanger.